Design of an Optical Sensor to Detect Human Intestinal Bleeding for Capsule Endoscopy

A Thesis Submitted to the College of Graduate and Postdoctoral Studies

In Partial Fulfillment of the Requirements

For the Degree of Master of Science

In the Department of Electrical and Computer Engineering

University of Saskatchewan

Saskatoon SK, Canada

By

Alimul Haque Khan

Permission to Use

In presenting this thesis in partial fulfillment of the requirements for a Postgraduate degree from the University of Saskatchewan, I agree that the Libraries of this University may make it freely available for inspection. I further agree that permission for copying of this thesis in any manner, in whole or in part, for scholarly purposes may be granted by the professor or professors who supervised my thesis work or, in their absence, by the Head of the Department or the Dean of the College in which my thesis work was done. It is understood that any copying or publication or use of this thesis or parts thereof for financial gain shall not be allowed without my written permission. It is also understood that due recognition shall be given to me and to the University of Saskatchewan in any scholarly use which may be made of any material in my thesis/dissertation.

Requests for permission to copy or to make other use of the material in this thesis in whole or part should be addressed to:

Head of the Department of Electrical and Computer Engineering

57 Campus Drive

University of Saskatchewan

Saskatoon, Saskatchewan S7N 5A9, Canada,

OR

Dean

College of Graduate and Postdoctoral Studies

University of Saskatchewan

116 Thorvaldson Building, 110 Science Place

Saskatoon, Saskatchewan S7N 5C9, Canada.

Abstract

Gastrointestinal (GI) bleeding in human is not uncommon that may sometime lead to fatal consequences. Types of GI bleeding include acute and chronic bleeding, upper and lower bleeding. In some cases, the patient requires immediate diagnosis. These abnormalities could be detected by using a flexible wired endoscope, a tool to see inside view of the GI tract. An advanced version of endoscopy tool is the wireless capsule endoscopy (WCE), first used in 2001, where the patient swallows an electronic capsule-shaped device which captures thousands of images and sends to an external data recorder via wireless communication. The images are later analyzed by physicians to detect GI abnormalities. The screening process is time-consuming. Delay in bleeding detection may increase the risk of the patient. Therefore, an easy and faster way to detect bleeding in the GI tract by using optical sensors is warranted.

Standard methods to diagnose GI bleeding are still limited due to unpredictable bleeding behaviours, such as the rate of bleeding and the concentration of blood. In addition, proper instrumentation, lack of easy access and control of the sensors are also limiting the techniques of bleeding detection. Blood can be identified by analyzing its optical properties. To determine its optical properties, three types of experiments using a spectrophotometer, a pulse oximeter, and an RGB colour sensor were conducted in this research. The principle is to emit light of a specific spectrum from a source on a liquid sample. Depending on the protein (like hemoglobin) or other substances present in the liquid, a different wavelength of light will be reflected and/or transmitted, which is then detected using a sensor (typically the photodiode).

The objective of this study is to distinguish blood samples (BS) from non-blood samples (NBS) using their optical properties. Different concentrations of horse blood, swine blood, and

bovine hemoglobin solutions were used in this experiment as BS. Many other solutions like coffee, tea, juice, coloured water, etc. were used as NBS. One set of data samples was first used to develop the algorithm. Next, another set of samples was used to validate it.

Several wavelengths of the light spectrum were identified in the study. Analysis of the experimental results suggests that it is possible to separate BS from NBS using the optical properties of the substances. The outcomes of this study can be used to implement small optical sensors in a capsule endoscopy system to detect GI bleeding. The optical sensor will eliminate the post-processing of the images and thus save a significant amount of time.

Acknowledgements

At first, I gratefully praise to Almighty God for enabling me to complete my thesis work. I would like to express my most gratitude and appreciation to my supervisor, Dr. Khan A Wahid, for his continuous support and encouragement throughout the work. It was quite impossible for me to complete this work without his valuable expertise, advice, and encouragements.

Special thanks to Professor Julia Montgomery of Western College of Veterinary Medicine and Raelene Petracek of Prairie Swine Centre Inc. for providing blood samples to conduct the experiments. I am also thankful to all my lab colleagues who helped me a lot in conducting the experiments.

Finally, I would like to express my thanks to wife and parents for their mental support to complete my study.

Table of Contents

List of Tables

List of Figures

Abbreviations

ATL	Amount of Transmitted Light
ARL	Amount of Reflected Light
BS	Blood Samples
CWE	Conventional Wired Endoscopy
EDTA	Ethylene-Diamine Tetra-acetic Acid
GI	Gastrointestinal
HSL	Hue, Saturation, Lightness
IR	Infrared
LED	Light Emitting Diode
NBS	Non-blood Samples
RGB	Red, Green and Blue
RBC	Red Blood Cell
WBC	White Blood Cell
WCVM	Western College of Veterinary Medicine
WCE	Wireless Capsule Endoscopy

Chapter 1 Introduction

1.1 Gastrointestinal Bleeding

Gastrointestinal (GI) bleeding is any types of bleeding that occurs in human GI tract [1]. In some cases, it can be a life-threatening issue if not diagnosed and treated properly in time. Depending on the rate of blood loss, GI bleeding can be classified as overt and occult bleeding. The amount of bleeding may be massive for short time which is known as overt bleeding. This is visible and also known as acute bleeding. Occult bleeding is the result of microscopic hemorrhage with no visible blood loss noticed by the patient or physician, which is also known as chronic bleeding. In this case, a small amount of bleeding may continue for a long time [2].

Depending on the source of bleeding, GI bleeding can be categorized as upper GI bleeding and lower GI bleeding. Sometimes, the source of GI bleeding is difficult to locate, which is termed as obscure GI bleeding. It could be either overt or occult bleeding, or upper or lower GI bleeding. Obscure GI bleeding refers to the recurrent bleeding in which the source of bleeding is not identified after upper endoscopy and colonoscopy [2].

Based on the symptoms of abnormalities, the clinicians perform different medical tests to confirm the nature and source of the bleeding[3], [4]. One of the procedures to detect GI bleeding is to use an endoscopy. The endoscopy is also used to identify celiac disease, inflammation, swelling, ulcers, bleeding, tumours, lesions, precancerous abnormalities, and blockages [5] [6] [7]. However, conventional endoscopy contains a camera mounted with a cable which is used to deliver power to the camera and communicate with a workstation. This makes the endoscopy uncomfortable and painful. Moreover, the device is also limited to travel within the stomach and duodenum of the whole GI tract. On the contrary, the wireless capsule endoscopy (WCE), a tiny

electronic device and an advanced version of traditional endoscopy, has overcome these limitations [8]. This device is available in the market since 2001[9].

WCE can be used to detect abnormalities by analyzing the captured images. However, the images captured by WCE is huge in number and thus the manual diagnosis of bleeding is time-consuming and inefficient [7], [10]–[13]. Computer-aided diagnosis (CAD) offers a solution to this issue [7], [14]–[16]. Still, there is a time gap between image capture and abnormalities identification, as the diagnosis process cannot be started while the device is inside the patient's body. In this context, a sensor-based system could be integrated with or substituted to the existing image sensor-based system. Appropriate sensors could be used to detect the presence of blood in GI tract that might reduce the post-analysis time of the images [17].

1.2 **Capsule Endoscopy**

In medical terminology, the capsule endoscopy is a procedure to observe inside of the GI tract especially the esophagus, stomach, small intestine, and colon [18], [19]. Based on the region and the application of the endoscopy, it has further been categorized as cystoscopy, colonoscopy and a few other types [20]. In 1806, Phillip Bozzini, known as "Father of Endoscopy", demonstrated light conductor (Lichtleiter) that enabled the direct view into the living body [21], [22]. The term "endoscopy" was first used by Antonin Jean Desormeaux in 1853 [19]. "Fibrescope", an optical unit that conveyed optical images along a flexible axis, was developed in 1954 [23]. In 1955, a French team of bronchoscopists broadcasted their endoscopic technique on live television[24]. The endoscopic system was developed further by many physicians and technologists, and now the whole procedure is miniaturized to include tiny camera/s and lighting apparatus, communication module and processor[13][25][26].

Through the conventional wired endoscopy (CWE), a physician can control the position of the camera and thus locate the abnormalities without much difficulty. However, the region of operation of CWE is limited within the duodenum or the colon[27]. In addition, due to pain/discomfort of inserting the wire and accessories of the endoscopy, a smaller and wireless version of endoscopy is always a topic of research[28].

The first wireless device to send information from GI tract was introduced by Dr. V. K. Zworykin in 1957. It was named as "Radio Pill" and comprised of a plastic capsule which was 1.125 inches in length and 0.4 inches in diameter. It transmitted signals according to the variation of pressure in GI Tract [29].

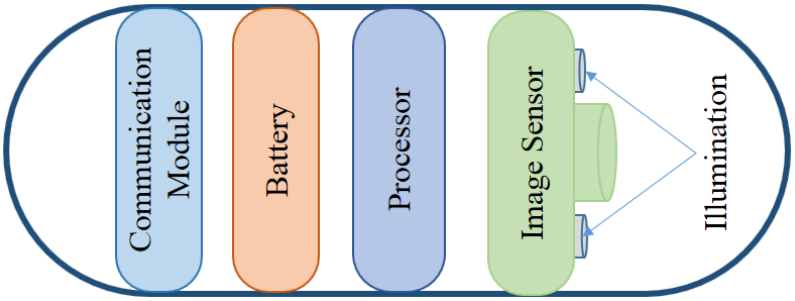

Figure 1-1: A typical block diagram of a wireless capsule endoscopy

Microelectronic development, condensed batteries, and efficient technologies made it possible to turn the whole system into a capsule [30][27]. A complete capsule endoscopy with self-illumination, camera, battery, processor, and transmitter was introduced in 2000 by a company named Given Imaging [9]. It needs a data recorder to receive data from the capsule. A Typical Block Diagram[31] of a Wireless Capsule Endoscopy (WCE) is shown in Figure 1-1

Capsule Endoscopy has been developed over the last 17 years, and several companies have introduced their capsule endoscopy with competitive designs and features [32] [33]. The capsule sends the captured images to the data recorder through appropriate wireless communication. The

outputs can be observed directly on the data recorder or can be downloaded to a workstation later. The outputs are then analyzed, and the abnormalities are diagnosed based on the analysis. A complete system of how WCE works is shown in Figure 1-2.

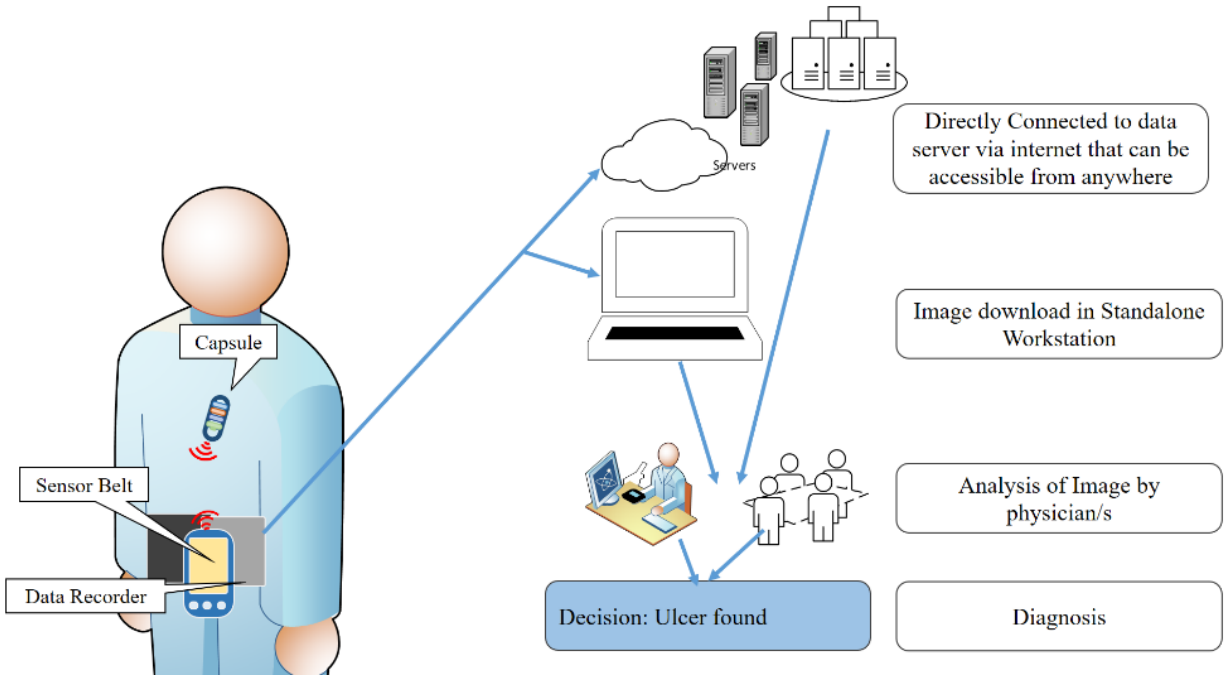

Figure 1-2: A complete system of wireless capsule endoscopy

The first capsule endoscope released by Given Imaging was PillCam SB, focusing mainly on the small bowel. Further, the company introduced PillCam ESO to view the esophagus, and PillCam Colon to examine the colon. Besides these, Given Imaging also released some updated version of its products such as PillCam SB 2, SB 3, ESO 2, ESO 3, Colon 2. Along with Given Imaging, few more companies also brought their products to the market such as Intromedic, Olympus, JinShan Science and CapsoVison. Each product has its own feature and specialty [34] [35] [36]. A short comparison of the products is shown in Table 1-1.

Table 1-1: Comparisons of capsule endoscopy available in the market (the latest version)

Device	PillCam SB	PillCam ESO	PillCam Colon	MiroCam	EndoCam	OMOM	CapsoCam
Company	Given Imaging			Intromedic	Olympus	JinShan	CapsoVision
Region of Operation	Small Bowel	Esophagus	Colon	Small Bowel	Small Bowel	Small Bowel	Small Bowel
Dimension(mm)	11 x 26	11 x 26	11 x 31	10.8 x 24.5	11 x 26	13 x 27.9	11 x 31
Mass (gm)	3.0	2.9	2.9	3.25	3.3	≤6	4
Battery life	≥8 hr	0.5 hr	10 hr	12 hr	12 hr	8 hr ±1 hr	~15 hr
Filed of view	156°	172°	172°	170°	160°	140° ±10	360°
Frame rate	2 or ~6	35	4 or 35	3	2	0.5 or 2	3 or 5
Image sensor	1 CMOS	2 CMOS	2 CMOS	1 CMOS	1 CCD	1 CMOS	4 COMS
Transmission	RF	RF	RF	HBC	RF	RF	USB
Real Time	Yes	Yes	Yes	Yes	Yes	Yes	No

RF: Radio Frequency; HBC: Human Body Communication; USB: Universal Serial Bus

1.3 Limitation of Existing Capsule Endoscopy

The capsule Endoscopy technology has advanced greatly, but there are still some major limitations [6], [9], [13], [25], [27], [28], [37]–[44]. One of the limitations is to control the movement of the capsule. As the capsule moves due to the natural movement of the GI tract, the physician cannot control its position as they can do it in wired endoscopy. In case of wired endoscopy, a physician can focus on the region of interest by controlling its position. However, in case of WCE, controlling the position is still in research. Few other limitations of WCE are collecting tissue samples and drug delivery into specific points of the GI tract which is now possible by the cable based endoscopy [13]. To overcome these limitations, it is necessary to

design smaller sensors and actuators for position control and sample collection. It is also necessary to incorporate them into the capsule endoscopic system in such a way that the device still remains swallowable.

Along with the localization and visualization of the GI tract, few GI parameters such as GI tract pH, luminal pressure and temperature, and gastric emptying time are also important to diagnose diseases and abnormalities. These parameters could be determined by using various sensors. For example, Given Imaging has introduced several sensors such as temperature sensors, pressure sensors, and pH sensors in SmartPill, a variation of capsule endoscopy [37][45].

In the current technology, diagnosis of abnormalities from the images needs post-examinations of the images. To make the diagnosis easier, computer-aided detection is becoming popular nowadays [14] [16]. However, the post-processing of the images still requires time as it starts after completing the whole endoscopic procedure, therefore, immediate diagnosis is not possible. Delay in the detection of GI bleeding could lead a patient to death [46]. These issues could be solved by using different types of sensors which could send real-time information about the bleeding detection. Bleeding in GI tract could be detected by analyzing the optical properties of blood.

Blood contains hemoglobin that makes the colour of blood reddish. Redness also depends on the level of oxygen saturation. Oxygenated blood is bright reddish whereas deoxygenated blood is dark reddish in colour. Colour is an optical property that could be used to determine the presence of blood in GI tract. Some of the optical properties are absorption coefficient, transmittance, reflectance, and scattering coefficient. The properties mainly depend on the wavelengths of the incident light and the subject of the experiment [47] [48] [49].

The required optical properties could be measured by light sensors such as 'photoresistors', 'photodiodes', and 'phototransistors' which are the electronic components that change their behaviour according to the intensity and wavelength of light. The behaviours of the reflected, transmitted or scattered light depend on the medium, molecular structure of the object and its surface, and on few other physical properties [50]. There are some standard methods to measure these properties [51]. The properties vary for different substances and hence, blood shows different characteristics from other substances. Analysis of the properties using different light sensors at certain wavelengths could show the differences between blood and non-blood substances. Therefore, the differences of the properties could be used to detect the blood and bleeding in the GI tract. As the sensors and other accessories are becoming smaller, these could also be integrated into the capsule for bleeding detection[17].

Literature indicates that the infrared and red light and the RGB sensor could be used to detect the GI bleeding. However, the range of the blood concentration that can be separated from non-blood samples by their research work was limited within small ranges. Also, the number of samples used in for experiments were less than 30. The proposed designs can measure only the blood which enters the designed hole of the capsule. It cannot read any sample that does not enter into the hole, for example, the blood attached to the GI wall.

1.4 **Thesis Objective**

The goal of this thesis is to find the optical sensors that can be used to differentiate GI blood from other substances and integrated with a wireless capsule endoscopy system. To achieve the goal, the following three research objectives are set:

a. To explore the spectrum of wavelengths at which the blood and non-blood samples show the best separation. These experiments were carried out by a spectrophotometer.

b. To explore the relationship/s between the amount of the transmitted infrared and red light through samples to distinguish the samples based on that relations.

c. To examine the relationship/s among the value of red, green and blue channel of the RGB sensor to differentiate blood and non-blood sample.

1.5 Thesis Organization

The thesis consists of eight chapters. Chapter 2 presents about GI bleeding characteristics and possible sensors to detect that. In Chapter 3, discusses the samples used in this study. Chapter 4 describes the analysis of the samples by using a spectrophotometer, Chapter 5 discusses the analysis of the samples by using a pulse oximeter sensor, and Chapter 6 discusses the analysis by using an RGB sensor. Summary of the accomplishment and comparison with the literature are presented in Chapter 7. Finally, chapter 8 concludes this thesis along with some recommendations for future directions to this work.

Chapter 2 Research Background

2.1 Characteristics of Blood

The blood is a body fluid that delivers nutrients and oxygen to the body cells and transports metabolic waste products from the cells. The blood consists of red blood cell (RBC), plasma, and white blood cell (WBC) in the amount of 45%, 54.3% and 0.7% respectively [52]. RBC is also known as erythrocyte that contains hemoglobin. It is a protein inside the RBC that carries oxygen.

Blood is red in colour due to the presence of hemoglobin. The colour of blood also depends on the oxygen saturation of blood. The oxygenated blood is bright red (arterial) and the deoxygenated blood is dark red (venous) [52] [53]. Thus, the oxygen saturation plays an important role in spectrophotometry of blood. The optical properties such as reflection, scattering, transmission hence depend on the percentage of oxygen saturation.

The erythrocyte is discoid in shape and it has very strong light scattering and absorption properties. The optical properties of blood are dominated by the presence of RBC, hence these properties are also highly dependent on the dilution of blood [54].

2.2 Sensors used in Capsule Endoscopy

The sensor is an electronic component, module or subsystem that converts any events or changes of physical environment into signals, especially electrical signals. Depending on the characteristics, sensors may be categorized into different types such as the pressure sensor, temperature sensor, velocity sensor, optical sensor and many more. Any event, change or state can be expressed by an electrical signal by using appropriate transducers which converts that event/state into an electrical voltage or current. The only sensor itself cannot make a complete

system. Other peripheries are required to build a complete system along with the sensor. Normally, the outputs of the sensors are analyzed, and actions are taken based on the analysis[55]. Wireless medical devices that sense different physiological parameters are becoming popular day by day [56]–[58].

The sensors used in SmartPill (Given Imaging) are the temperature sensor, pressure sensor, and pH sensor. The outputs of these sensors provide important parameters of the GI tract [59]. CorTemp and VitalSense are some of the capsules which use to measure the internal body temperature [60] [61]. These ingestible temperature sensors are used mainly to measure the heat stress in patients and workers in the industrial environments, and also possibly soldiers in the field. The pH of GI juice varies with the location of the GI tract. The measurement of pH provides an idea about the transit time of the capsule and food. Bravo pH another product of Given Imaging also measures pH [62]. The pressure sensor is also used in those capsules although accurate pressure profile for the GI tract is yet to be discovered[63]. Besides these sensors, optical sensors to detect bleeding in the GI tract are in research [42], [64]–[66].

Information from the GI tract could be sensed by appropriate sensors [33] [67]. Peristalsis movement, pressure, temperature, pH, gas profile, colour, pattern, shape, acoustic environment and many other parameters of the GI tract could be used to identify the abnormalities and their locations. For example, the abrupt change in pH profile of the GI tract could be used to ensure that the capsule has left from the stomach[68]. However, detection of bleeding using sensor is still challenging. Considering the smaller space available for the sensors to detect bleeding, appropriate sensors and methods are the topics of intense research.

The sensors used in this research are basically the optical sensors. Depending on the way the sensor works, the names of the sensors are different such as the spectrophotometer measures

the reflection of light at different wavelengths, the pulse oximeter measures the transmission of red light and ultraviolet light, and the RGB colour sensor is used to measure the reflection in red, green and blue colour spectrum.

2.3 Previous Works on Blood Detection using Sensors

Few studies are available that describe the characteristics of blood by using spectrophotometer or colour sensor. The researchers are successful to distinguish the blood from non-blood samples using the characteristics to a certain extent [42], [64]–[66], [69]. However, a concrete idea to identify the presence of blood in GI tract has yet to be revealed.

An intelligent electronic capsule system has been examined in a project supported by some organizations in China, 2010. They used the TCS230D sensor which converts light wave into a square pulse train of the corresponding frequency. Thirteen different concentration of bovine hemoglobin (Sigma H2625) were used to find out the properties of blood. Two factors had been proposed by their experiment to detect the symptom of hemorrhage. This work lacks comparison between the outcome of hemoglobin solution with other substances that are similar to blood/hemoglobin or intestinal juice. The sample readings were measured by using the internal reflection of the light source while blood entered into the designed hole in the capsule [69].

A similar work has been done using two intestinal juice and normal human blood with different dilution in 2016 where a colour sensor, TCS 3200 was used. They used HSL (Hue, Saturation, and Lightness) colour recognition scheme in their experiment. A region was identified to differentiate blood (total 08 samples) and intestinal juice (total 02 samples) based on HS distribution plane. It was not able to detect all the blood samples properly. They also read the samples while entered into the designed hole[42].

Ovesco Endoscopy AG (European VECTOR project) designed HemoCop Telemetric Sensor System in 2012. They have gone through an in-vivo assessment with a novel sensor implant anchored to the stomach wall. They applied different liquids such as water, milk, tea, red wine, orange juice and few more items into the sensor through an endoscopic channel. The ratio of transmitted intensities of red light (720 nm) and violet light (415 nm) had been used as a single parameter to distinguish blood from other substances [65].

A similar theory was used in another experiment where a telemetric real-time sensor has been proposed to detect the acute upper GI bleeding. In this experiment, the red light and violet light were used by a spectrophotometer to determine the optical characteristics of blood, and LED (Light Emitting Diode) of red light and violet light were used later to compare the analysis LED with the analysis of spectrophotometer. They used diluted human blood and other liquids that are similar to the colour of blood. In their analysis, it is found that the ratios of transmitted intensities of the red light and violet light for blood samples were significantly higher than other liquids. However, they used a small range of dilution of the blood solution such as 0.1% to 50% of concentration. Moreover, the range of blood samples identified properly by their algorithm was also narrow. For example, the ratio for the blood samples with the concentration of 1% to 10% showed difference than non-blood samples whereas the blood samples with other concentrations were in the same range as of few other non-blood liquids [64].

HemoPill, a capsule developed based on the telemetric sensor capsule, was used for a volunteer case study. A volunteer test person consumed meals with and without the adjunct of his own blood at different times. The study was able to find out a relationship between the concentration of blood in stomach contents and the ratio of transmitted intensities of red light and violet light [66]. All the designs mentioned in [64]–[66] measured the reading using a hole or a channel in the capsule.

2.4 Methodology to Detect Blood by Using Sensors

The sensor must be enough small to be fitted inside a small capsule and should be able to differentiate blood from other substances properly. There are several types of standard test and testing device that measures the characteristics/parameters of blood outside of the GI tract. However, the testing devices are huge in physical size compared to the size of a capsule endoscopic device. In this case, measurement of the gross reflection or transmission could be done very simply with tiny devices. For example, gross reflection could be measured by emitting light and reading the intensity of reflected light where the light emitter and the reader both are on the same side. However, to measure gross transmission, the blood should stay in a space between the light emitter and the reader. Possibly that space would be a tiny hole thus it is a great concern whether the bleeding is enough to enter into that hole as used in the previous studies [42], [64]–[66], [69]. The reflection could be used to detect the blood on the GI wall or blood mixed with other elements of the GI tract.

The characteristics of each substance are different. Hence, blood shows different characteristics than other substances. The characteristics could be electrical properties, magnetic properties, optical properties or any other physical properties. The optical properties were used in this study to distinguish blood samples from non-blood samples. Three different instruments were used here to find out the optical properties of the samples.

The first one was a spectrophotometer that emits white light to a surface and measures the reflected intensity of light. It compares the intensity of reflected light to the intensity of emitted light in percentage for the visible light spectrum for example 400 nm to 700 nm. This device was directly connected to a computer to its own software interface, SpectraMagic NX. The data were exported to Microsoft Excel file and saved. The details of the working principle of the

spectrophotometer are provided in Chapter 4.

The second device was a pulse oximeter sensor. It emits red light and infrared light from one side of an object and measures the intensity of transmitted light from another side. Although this instrument is normally used to measure the oxygen saturation of blood, the same methods used in this hardware could also be used to measure the transmitted intensity of red light and infrared light. These two amounts could be used as optical properties to distinguish the blood and non-blood samples. The ratio of the intensity of transmitted infrared light to that of transmitted red light was used as a parameter to separate the samples in this study. This device was connected to a processor (Arduino Uno) that controls the red and infrared light sources and measures the received intensity of transmitted light sequentially. The processor was connected to a computer and the received data were saved in Microsoft Excel files. The details of the working procedure of this device are described in Chapter 5.

The third device in this study was an RGB colour sensor, HDJD S-822. It emits white light to an object and receives the reflected light through three different channels named as the red, green and blue channel. The emission of white light and measurement of reflected light were processed using Arduino Uno. The data were saved in Microsoft Excel Files in a computer. Details of the working procedure of RGB colour sensor are discussed in Chapter 6.

The collected data for each instrument were saved in a computer and prepared for further analysis. The analysis was done in MATLAB, a numerical computing environment. A simple block diagram of the analysis is shown in Figure 2-1. The first block represents the collection of blood samples and non-blood samples, the second block represents the experiments using three different devices, the third block represents the analysis using MATLAB, and the fourth block represent results of the analysis. Although the symbols used in the fourth block is same as the

pattern recognition and classification, no standardized pattern recognition or classification schemes were used in this analysis. Instead, characteristics of the samples in terms of optical properties were found out to separate (in other word classify) the samples so that implementation of the sensors could be easier.

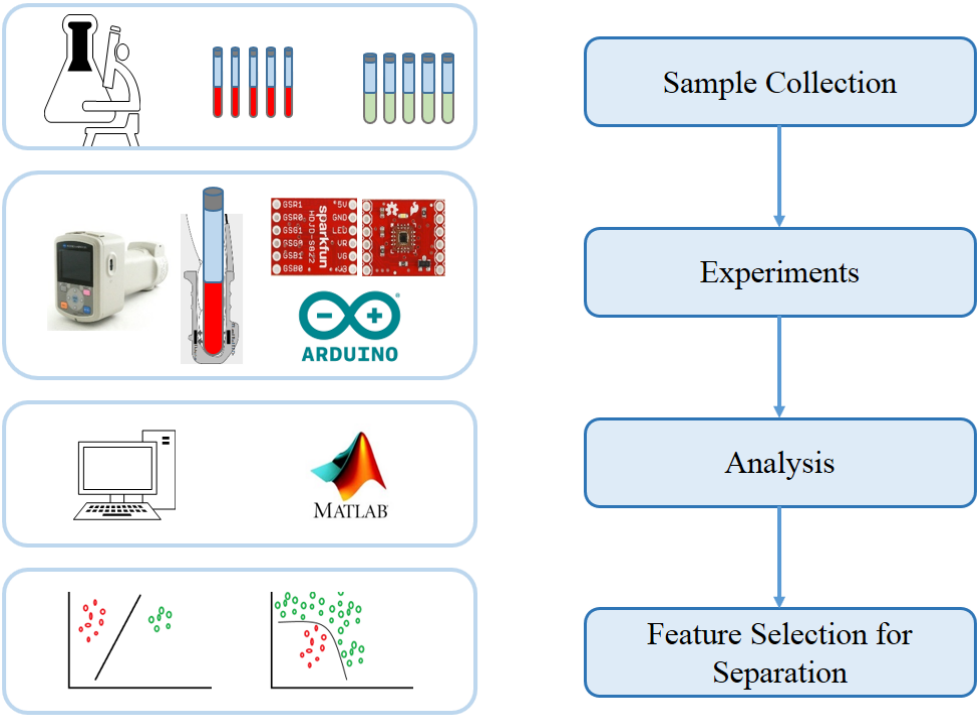

Figure 2-1: Simple block diagram of methodology of blood detection

Three different instruments were used in this study to separate blood samples from non-blood samples. The purposes were to explore some features/parameters of blood and non-blood samples with respect to these three instruments. The next chapter will discuss the procedure of sample collection and the datasets used for experiments.

Chapter 3 Sample Collection and Experiments

3.1 Test Procedure and Sample Collection

There are some regular activities for any endoscopic procedure [2]. Before conducting endoscopy, the patient needs to fast for twelve hours so that a clearer inside view of the GI tract could be attained. In a clearer view, the possible available substances that could be found in a normal GI tract are saliva, mucus, and few other digestive enzymes [70]. In case of any abnormality, blood or external substances may appear. The objective of this study is to differentiate blood from other substances by using different sensors. For this purpose, three different sensors were used in this study. For each sensor, two different datasets were utilized. Each dataset contained blood samples and no- blood samples. The blood samples included swine blood solutions, horse blood solutions, and bovine hemoglobin solutions. The non-blood samples included tea, coffee, juice, food colour, and different types curry and soups.

Figure 3-1 Few of the blood solutions with different dilution

All the solutions are kept in test tubes. The sizes of the test tubes were 5ml and 3ml. The horse blood samples were collected from healthy horse and diluted with proper anti-coagulant

agent and saline at Western College Veterinary of Medicine (WCVM), University of Saskatchewan. The swine blood samples were also collected in the same way from Prairie Swine Center. Bovine hemoglobin samples were made from crystallized bovine hemoglobin. Few of the blood solutions are shown in Figure 3-1.

3.1.1 Preparation of Horse Blood and Swine Blood Samples

Horse blood samples were collected at WCVM using vacutainer tubes containing an anti-coagulant agent (EDTA- ethylenediamine tetraacetic acid). Samples were then taken to the WCVM laboratory immediately where the samples were diluted with saline to 3mL samples. Duplicates for each dilution were made and one set of samples was sent to determine hemoglobin concentrations. The samples were then stored in the fridge until they were taken from WCVM to the laboratory of Department of Electrical Engineering, University of Saskatchewan. The swine blood samples were prepared in a similar way at Prairie Swine Center and taken for the experiment. The concentration of these samples was provided in the percentage of whole blood.

3.1.2 Preparation of Bovine Hemoglobin Samples

Sigma H2625 is the crystallized bovine hemoglobin which was used to prepare the hemoglobin solutions. First, the weight of an empty test tube was measured, then the weight of the test tube with bovine hemoglobin was measured. The difference between these two measurements was the mass of hemoglobin. Finally, water was poured into the test tube with proper measurement, and the top of the test tube was closed and shaken properly. The concentration of the solutions was calculated as gram per litre (g/L).

3.1.3 Preparation of Non-blood Samples

Different types of other solutions were used in this study as the non-blood samples. The samples included water, tea, coffee, juice, fruits, food colour, curry-soups and few other solutions.

3.2 Dataset

The datasets used in this study contained both blood samples and non-blood samples. Two different datasets were used in this study. The first one was used to develop a model to separate BS and NBS. It contained 22 blood samples and 13 non-blood samples. The second one was used to check the performance of the model developed using the first dataset. It contained 43 blood samples with 23 non-blood samples. The complete lists of these two datasets ate provided in Table 3-1 and Table 3-2.

Table 3-1: List of samples in the first dataset

Sample Number	Sample Description	Sample Number	Sample Description
1	Water	19	Horse blood -17%
2	Food colour-red	20	Horse blood -8%
3	Food colour-saffron	21	Horse blood -25%
4	Mango juice	22	Horse blood -50%
5	Cranberry juice	23	Swine blood -6%
6	Red grapes juice	24	Swine blood -30%
7	Black coffee (lower concentration)	25	Swine blood -40%
8	Black coffee (higher concentration)	26	Swine blood -70%
9	Black tea	27	Swine blood -80%
10	Aloe vera Pomegranate Juice	28	Swine blood -90%
11	Aloe vera Mango Juice	29	Swine blood -100%
12	Aloe vera Juice	30	Hemoglobin-19.4 g/L
13	Pepsi	31	Hemoglobin -22.8 g/L
14	Horse blood-58%	32	Hemoglobin -26.8 g/L
15	Horse blood -50%	33	Hemoglobin -37.4 g/L
16	Horse blood -42%	34	Hemoglobin -60.6 g/L
17	Horse blood -33%	35	Hemoglobin -70.2 g/L
18	Horse blood -25%		

Table 3-2: List of samples in the second dataset

Sample Number	Sample Description	Sample Number	Sample Description
1	Lentil Soup with water	34	Hemoglobin -32 g/L
2	Lentil Soup with less water than in sample 1	35	Hemoglobin -34 g/L
3	Lentil Soup with less water than in sample 2	36	Hemoglobin -29 g/L
4	Lentil Soup with less water than in sample 3	37	Hemoglobin -28 g/L
5	Lentil Soup with no water	38	Hemoglobin -39 g/L
6	Chicken Soup with water	39	Hemoglobin -16 g/L
7	Chicken Soup with No water	40	Hemoglobin -24 g/L
8	Chopped tomato with water	41	Hemoglobin -36 g/L
9	Chopped tomato with no water	42	Swine blood -0.04%
10	Milk and yogurt with red chili powder	43	Swine blood -0.1%
11	Milk and yogurt with turmeric powder	44	Swine blood -0.5%
12	Canola oil with turmeric powder	45	Swine blood -1.0%
13	Milk with chocolate syrup	46	Swine blood -2.0%
14	Chicken soup (Baked)	47	Swine blood -4.0%
15	Coffee 3 in 1	48	Swine blood -6.0%
16	Coffee 3 in 1 diluted	49	Swine blood -15%
17	Coffee 3 in 1 more diluted	50	Swine blood -25%
18	Chopped orange pill with water	51	Swine blood -40%
19	Crashed Tablet Vitamin C	52	Swine blood -50%
20	Orange juice extracted by hand	53	Swine blood -60%
21	Apple chopped	54	Swine blood -70%
22	Apple chopped with water	55	Swine blood -80%
23	Water	56	Swine blood -90%
24	Hemoglobin-6 g/L	57	Swine blood -100%
25	Hemoglobin -3 g/L	58	Horse blood -75%
26	Hemoglobin -7.6 g/L	59	Horse blood -67%
27	Hemoglobin -14 g/L	60	Horse blood -63%
28	Hemoglobin -14 g/L	61	Horse blood -50%
29	Hemoglobin -18 g/L	62	Horse blood -42%
30	Hemoglobin -12 g/L	63	Horse blood -33%
31	Hemoglobin -14 g/L	64	Horse blood -25%
32	Hemoglobin -12 g/L	65	Horse blood -8%
33	Hemoglobin -20	66	Horse blood -4%

3.3 Justification of Sample Selection

For both the dataset, the blood samples included different sources of blood such as horse blood, swine blood and bovine hemoglobin. The range of blood concentration was also varied in a wide range for example, from very low concentration to higher concentration of blood.

Table 3-3: The range of the concentration of blood samples

	First dataset	**Second Dataset**
Horse Blood	8% to 58%	4% to 75%
Swine blood	6% to 100%	0.1% to 100%
Hemoglobin	19.4g/L to 70.2 g/L	3 g/L to 39g/L

The wide range is taken to determine the range of concentration where the sensors work better or fail. The range of the concentration is shown in Table 3-3. The non-blood samples were also chosen mainly based on the fact that these samples should somehow mimic the colour of the gastrointestinal wall, and colour of blood. Moreover, some of the previous studies used similar NBS for their study.

Although the sensor is aimed to design to detect the human intestinal bleeding, the blood samples used in this study were collected from horse, swine. The hemoglobin samples made from bovine hemoglobin. The reasons behind not to use human blood samples are mainly due to the lack of available facilities in the works station, and the limited permission that allows only to hand the animal blood samples. As there are many similarities between the blood of human and other mammals such as the presence of hemoglobin and other blood components. Hence, it is expected that the result of the analysis using animal blood samples would be similar to that of human blood.

Chapter 4 Analysis with Spectrophotometer

The objective of this experiment was to investigate the wavelengths or the range of wavelengths in the light spectrum that could be used to distinguish the blood samples and the non-blood samples. The focus of this part of the study was to find out the maximum separation between BS and NBS by using different wavelengths of the spectrum. The experiment is carried out by a spectrophotometer. In this chapter, preliminary discussion about the spectrophotometer, its working principle, and the procedure of data collection by spectrophotometer are discussed first. Then, the analysis of the first dataset is presented. The algorithm developed using the first dataset is applied to the second dataset and the results are described finally.

4.1 Spectrophotometer

The spectrophotometer is an apparatus that measures the intensity of emitted/reflected light from an object, transmitted light through any substance and few other optical properties[71]. There are few essential parts of this device such as a light source that produces light, a filter that allows only a certain portion of the light spectrum, and a detector (photometer) that measures the intensity of reflected or transmitted light.

The spectrophotometer reads the amount of reflected light as the percentage of incident light. For a white surface, it is ideally 100% and for a black surface, the value is ideally 0% at each wavelength. However, the substances other than black or white surface show different amount of transmitted light at different wavelengths. This device is directly connected to a computer where all the experimental data can be saved. The data are then analyzed by appropriate software.

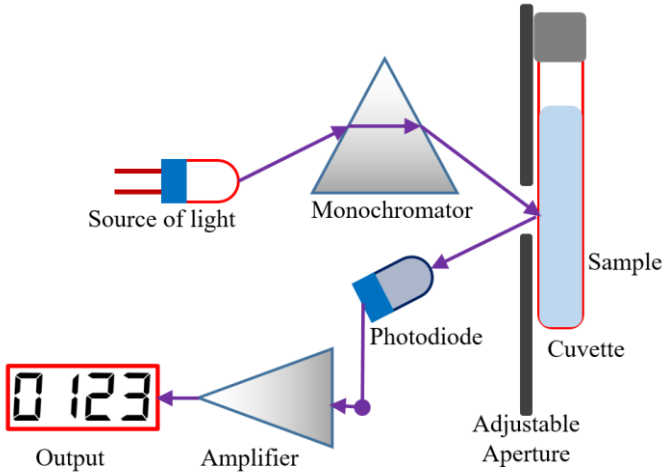

Figure 4-1 Basic working principle of a spectrophotometer

4.1.1 Working Principle

The spectrophotometer emits a light spectrum of a certain wavelength to the samples. Based on the arrangement of the detector and the emitter, this instrument measures the emitted/reflected amount of light from a sample or the transmitted amount of light through a sample. The detector could be photo-resistor, photodiode or phototransistor. Figure 4-1 shows how the intensity of reflected light is measured by spectrophotometer[72]. The spectrophotometer used in this study is KONICA MINOLTA SPECTROPHOTOMETER CM-600d which is shown in Figure 4-2. It uses pulsed xenon lamp with an ultraviolet cut filter as the light source and measures the intensity of reflected light by silicon photodiode array (dual 36 elements). The working range of this instrument is 400 nm to 700 nm with a pitch of 10 nm. The detailed specification is given in [73], [74].

Figure 4-2: Spectrophotometer (model # CM 600d) used in the experiment

The spectrophotometer is calibrated as “Zero Calibration” where the amount of reflection is almost 0% and “White Calibration” where the amount of reflection is almost 100% for the whole range (400 nm-700 nm). A white object ideally reflects all the light components incident on its surface hence, the reflection is 100%. On the other hand, a black object absorbs all components of the spectrum thus the reflection is 0%. An object with other colours absorbs all colour components other than its own colour and reflects only its own colour. Hence, the amount of reflected lights is different for each wavelength such as a red object shows higher value at around 670 nm whereas blue object shows higher value at around 500 nm of the spectrum. The operation of reflection measurement by this spectrophotometer is shown in Figure 4-3 [75].

The blood contains hemoglobin for which blood looks reddish. The colour is also dependent on the level of oxygen saturation of hemoglobin. Moreover, the structure of hemoglobin plays an important role in the interaction of blood with light. When the spectrophotometer emits white light on blood samples, a portion of the light is transmitted, absorbed, scattered and reflected. The amount of reflection is measured against the wavelengths of 400 nm to 700 nm with an increment of 10 nm such as 400 nm, 410 nm, 420 nm, …, 680 nm, 690 nm, 700 nm.

Figure 4-3: Operation of spectrophotometer, measuring the amount of reflected light

Other substances have different optical characteristics than that of blood and hence, the amount of reflection is dissimilar to those substances. The pattern of the reflected spectrum is used to differentiate the blood samples from the non-blood samples. However, instead of using the whole spectrum, a function of few wavelengths of the spectrum could optimize the decision-making parameter easier.

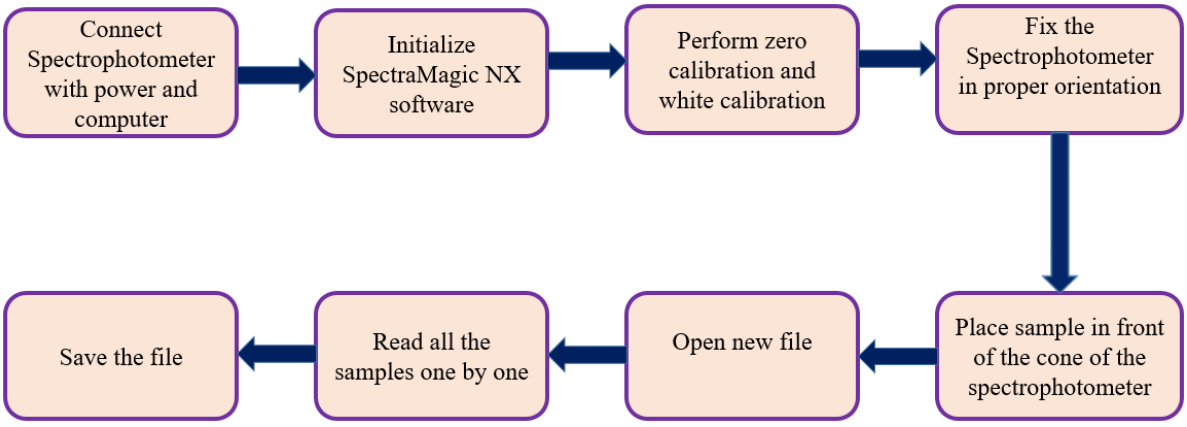

Figure 4-4: Flow chart of spectrophotometer experiments

4.1.2 Procedure of Data Collections

The experiments of spectrophotometer started with the connections of a power source. The device was also connected to a computer where the data were saved. SpectraMagic NX is the software provided by KONICA MINOLTA. This software provides the interface between the computer and the spectrophotometer. The details of the procedure are provided in its manual [76]. The samples were placed in front of the spectrophotometer with proper orientation and all the data were saved one by one. The whole process is shown in Figure 4-4. The saved data was copied to Microsoft Excel and analyzed in MATLAB later.

4.2 Analysis of First Dataset with Spectrophotometer

A total 3 readings were taken for each sample of the first dataset and then the mean was used in the analysis. The amount of reflected light at different wavelengths varied for different substances. Spectral response of hemoglobin, blood and all other solutions are shown in Figure 4-5. Hemoglobin solutions and blood solutions are presented as Blood Samples (BS) by red lines and other solutions are presented as Non-Blood Solutions (NBS) by green lines in this figure. For better readability, the detailed legends are not shown in this figure. As the main focus of the study is to explore the properties to separate the blood samples from non-blood samples, all the samples are shown only by using two legends. Moreover, each sample was normalized comparing with the water sample shown in the vertical axis. Hence, many of the samples have value more than 100 and reading for water is 100 for all the wavelengths.

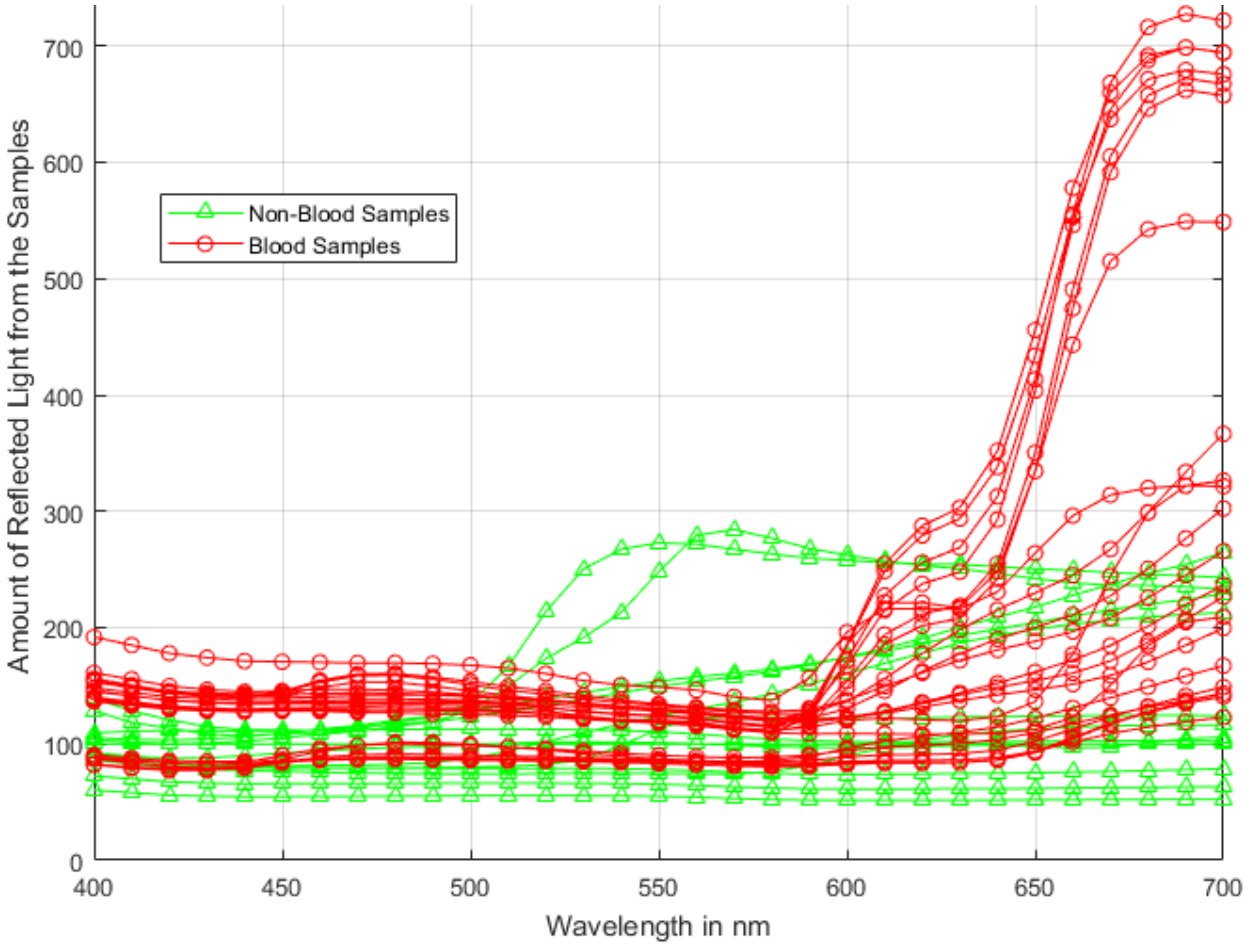

Figure 4-5: Reflected intensity of different samples.

The figure illustrates that the blood samples show higher value at the region of 670 nm than at other wavelengths and lower slope at around 630 nm. However, few samples of blood solutions are very close in spectral response with the other solutions. The detailed analyses are discussed in the next subsection.

4.2.1 Development of the Algorithm

The spectral responses of the samples are shown in Figure 4-5 but it looks clumsy and therefore it is hard to make any decision based on the plot. The range of the spectral response is

400 nm to 700 nm with a wavelength segment of 10 nm. Hence, the output of the device for one sample had 31 values from 400 nm to 700 nm with the step size of 10 nm. The spectral response of any sample *n* could be defined as:

$Response_n = F(\lambda_1, \lambda_2, ..., \lambda_{31})$ ---------- (4-1)

The objective of the study using the spectrophotometer is to differentiate BS and NBS mostly. Instead of using all the wavelengths, a minimum number of wavelengths should be used for simple and easier implementation of the outcomes in the CWE. Figure 4-5 suggests that the ratio of the amount of reflected light (ARL) at two different wavelengths could be used to differentiate the samples. Moreover, few of the previous study also suggests the ratio at two different wavelengths as a parameter to separate the samples [64]–[66].

The Ratio of ARL at two wavelengths (λ_a, λ_b), for any sample *n,* could be expressed as

$R_n (\lambda_a, \lambda_b)$ = ARL at λ_a for sample n/ ARL at λ_b for sample n -------- (4-2)

In the initial stage of the study, the samples were grouped according to their similarities. The ratios for BS and NBS at two wavelengths ((λ_a, λ_b) were expressed as:

Ratio of BS $(\lambda_a, \lambda_b) = [R(BS_{G1}), R(BS_{G2}), R(BS_{G3}), ... , R(BS_{Gp})]$ -------- (4-3)

Ratio of NBS $(\lambda_a, \lambda_b) = [R(NBS_{G1}), R(NBS_{G2}), R(NBS_{G3}), ... , R(BS_{Gq})]$ -------- (4-4)

The range of the ratio of the grouped samples and the separation could be expressed as:

Range of the ratio of BS (λ_a, λ_b) = [minimum (BS) maximum (BS)] -------- (4-5)

The range of the ratio of NBS (λ_a, λ_b) = [minimum (NBS) maximum (NBS)] -------- (4-6)

Separation (λ_a, λ_b) = minimum (BS)-maximum (NBS) -------- (4-7)

The negative value of separation means the overlap in range among the samples, and positive value signifies the separation. The separation is set as zero if the value of separation is negative, as there is no concern about the region of overlap. Each sample is a function of the values

of reflection at 31 different wavelengths. Therefore, the separation is calculated for all the possible pairs of wavelengths. The values of separation could be expressed by 31x31 matrix as shown in the matrix below:

SEPARATION=

$$\begin{bmatrix} Separation(\lambda 1,\lambda 1) & Separation(\lambda 1,\lambda 2) & \cdots & Separation(\lambda 1,\lambda 30) & Separation(\lambda 1,\lambda 31) \\ \vdots & & \ddots & \vdots & \\ Separation(\lambda 31,\lambda 1) & Separation(\lambda 31,\lambda 2) & \cdots & Separation(\lambda 31,\lambda 30) & Separation(\lambda 31,\lambda 31) \end{bmatrix}$$

---------- (4-8)

The separation is illustrated in Figure 4-6. The vertical axis shows the separation between BS and NBS. Horizontal two axes show the wavelengths (λ_a, λ_b) as given in Equation (4-2).

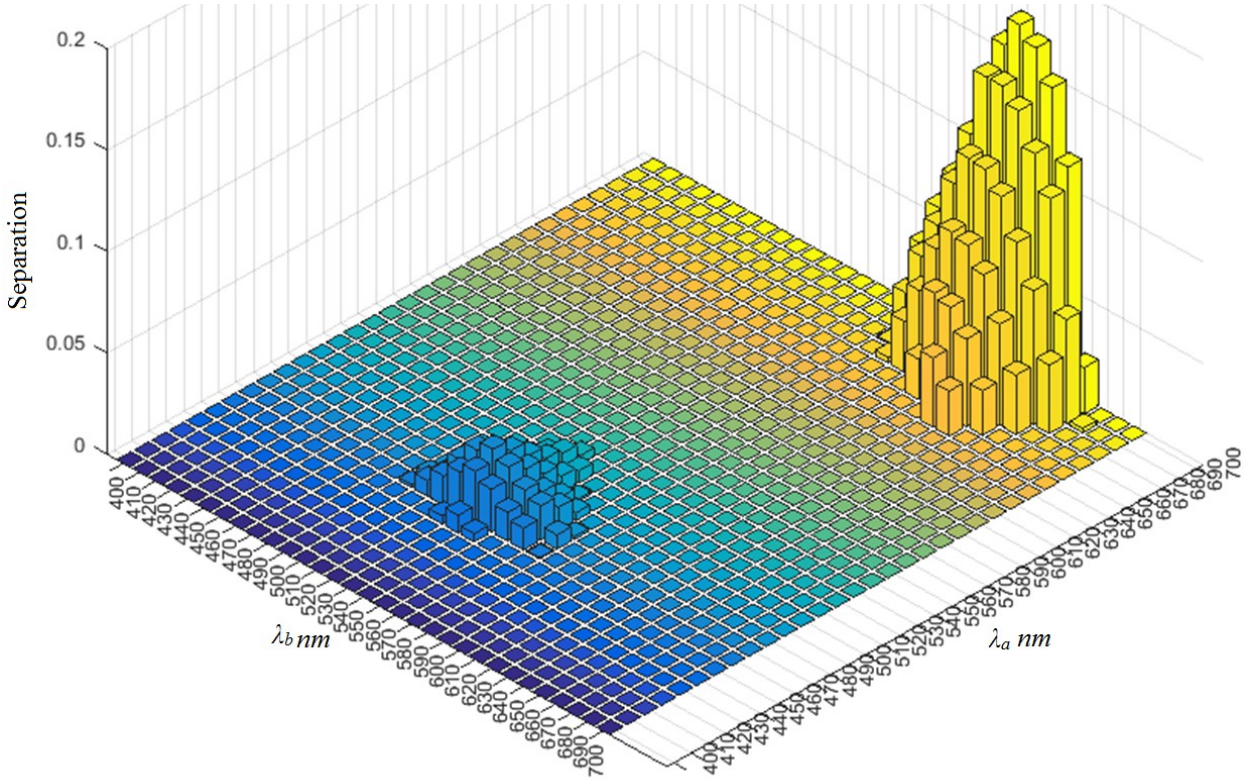

Figure 4-6: Separation between the ratio of ARL at two different wavelengths

Figure 4-6 shows two different regions where the separation is maximum. The first region is around (700 nm, 630 nm), and the second region is around (480 nm, 530 nm). A cut-off point was used to show the separation. The normalized ratio is calculated by subtracting the cut-off point from the ratio. The cut-off point is calculated using the mean of the median of BS and median of NBS.

Based on the preliminary analysis, the rest of the analyses were conducted. From now on, the term "ratio" will mean the ratio of the amount of reflected light for this chapter. The term "normalized ratio" will mean the ratio after subtracting the cut-off point. The samples that will be discussed to comment on the analysis are described in detail in Table 3-1 and Table 3-2.

4.2.2 Performance of the Algorithm on the First Dataset at (700 nm, 630 nm)

The primary analysis of this study suggests that the ratio at (700 nm, 630 nm) provides a good separation between BS and NBS. The ratios for the first dataset is shown in Figure 4-7. This figure shows that there are differences between the ratio BS and NBS. For BS, the ratio is little higher than that of NBS. Figure 4-8 shows the normalized ratio at the pair of wavelengths *(700 nm, 630 nm).* In this case, the cut-off point is found as *1.3664*. A clear separation between blood samples and non-blood samples is also revealed in Figure 4-8.

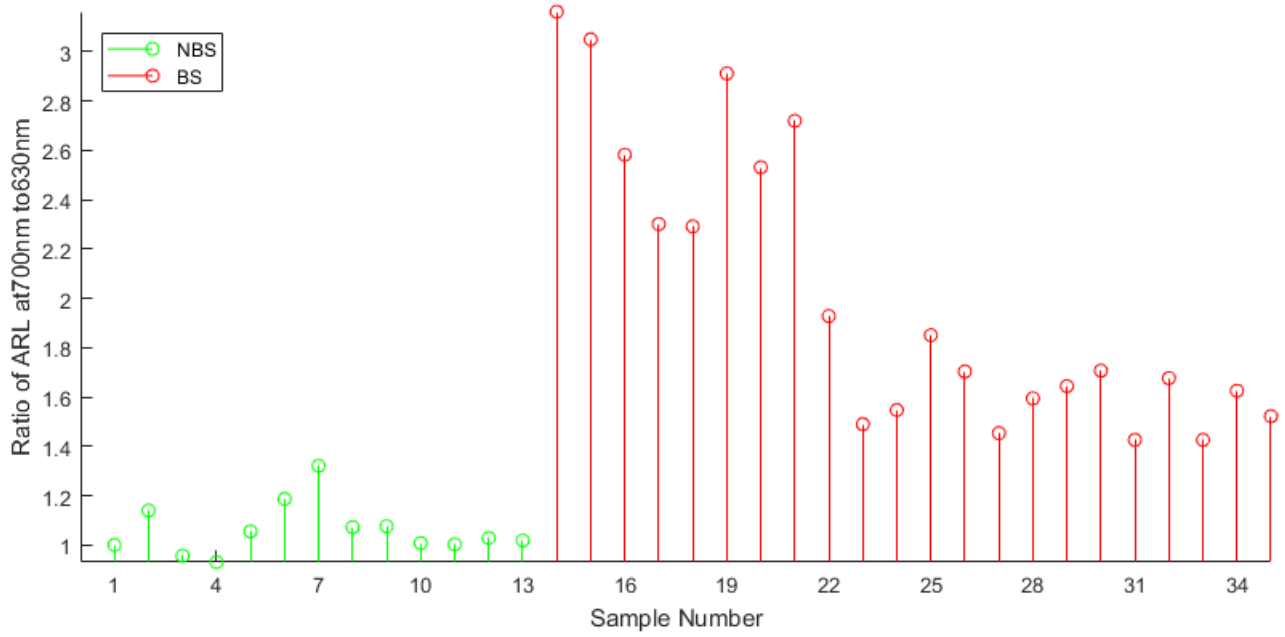

Figure 4-7: The ratio at (700 nm, 630 nm)

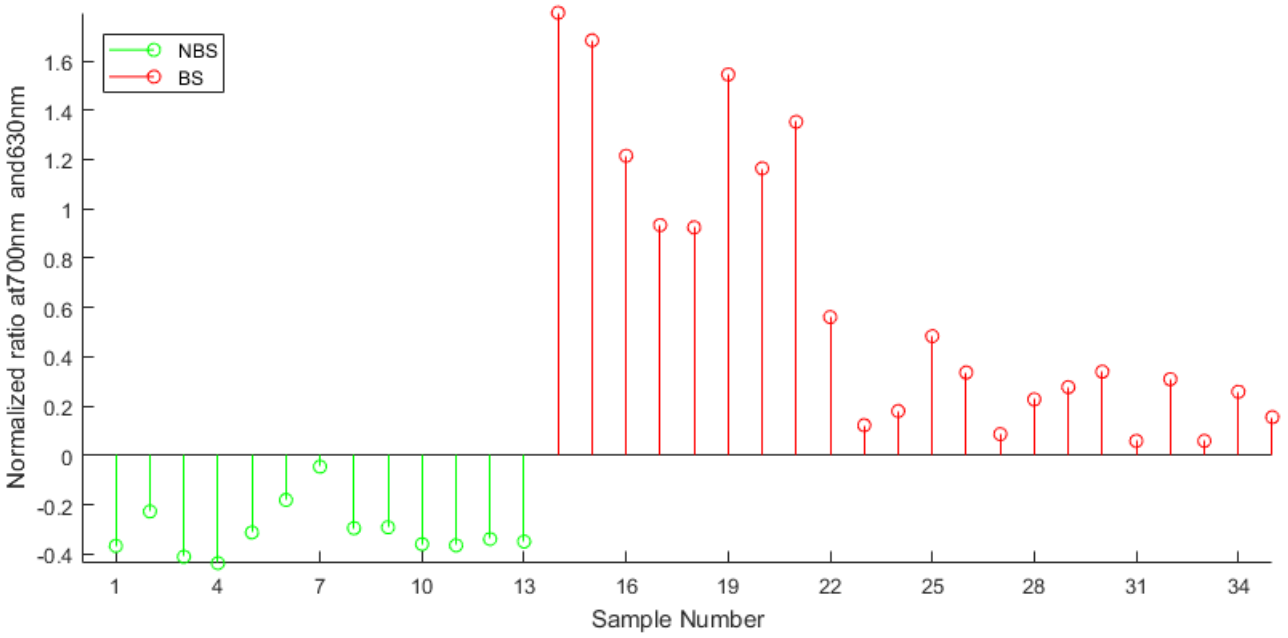

Figure 4-8: The normalized ratio at (700 nm, 630 nm)

Both Figure 4-7 and Figure 4-8 show the separation between BS and NBS. However, there are few BS and NBS which are very close to the cut-off point. For example, sample number 7 (black coffee with lower concentration) is very close to the separating line. Some samples of hemoglobin are also close to the separating line. However, all the samples are separated properly by using normalized ratio at (700 nm, 630 nm).

4.2.3 Performance of the Algorithm on the First Dataset at (480 nm, 530 nm)

Besides the ratio at (700 nm, 630 nm), the ratio at (480 nm, 530 nm) also provides similar separation between BS and NBS which is shown in Figure 4-9. The normalized ratio at (480 nm, 530 nm) is shown in Figure 4-10 where the cut-off point is found as 1.0095.

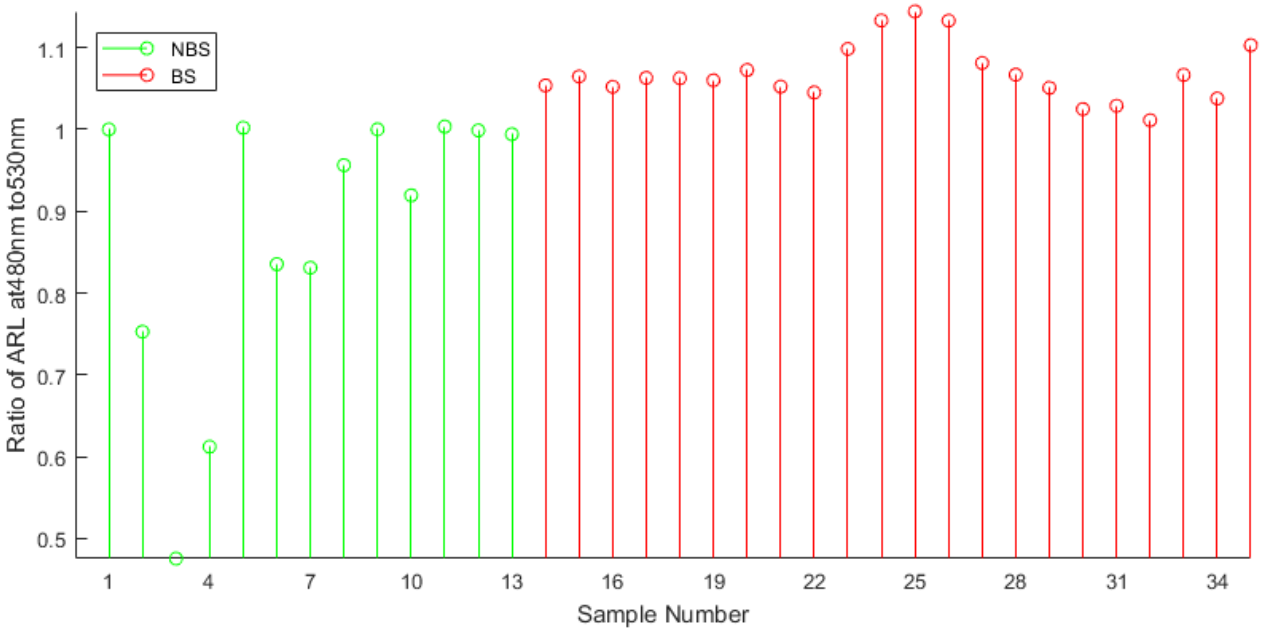

Figure 4-9: The ratio at (480 nm, 530 nm)

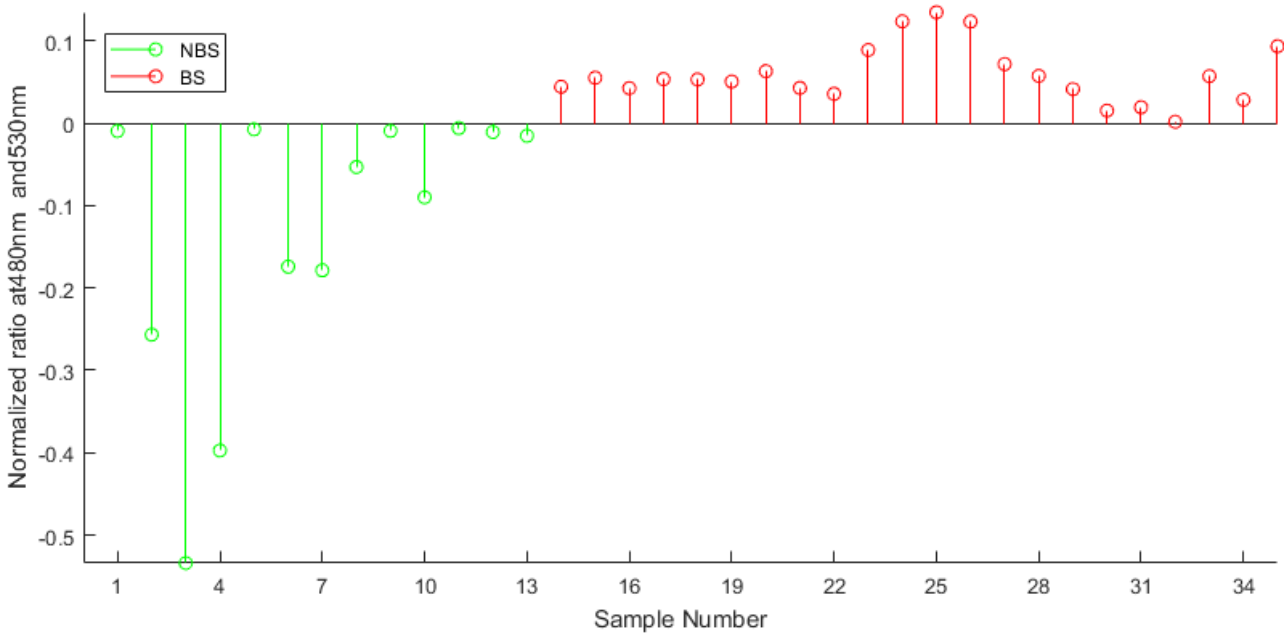

Figure 4-10: The normalized ratio at (480 nm, 530 nm)

The separation is achieved by using normalized ratio at (480 nm, 530 nm), although the amount of clearance is very small. The samples 1, 5, 9, 11,12,13,30, and 32 are very close to each other.

4.3 Validation of Analysis with the Second Dataset

A completely new dataset with similar samples was used as the second set of the samples. This set is used to verify the primary results of this study. The ratio was determined at various pairs of wavelengths especially those found by using the first dataset. Figure 4-11 and Figure 4-12 show the ratio at *(700 nm, 630 nm)* and the normalized ratio at *(700 nm, 630 nm)* where the cut-off point is found as 1.2093.

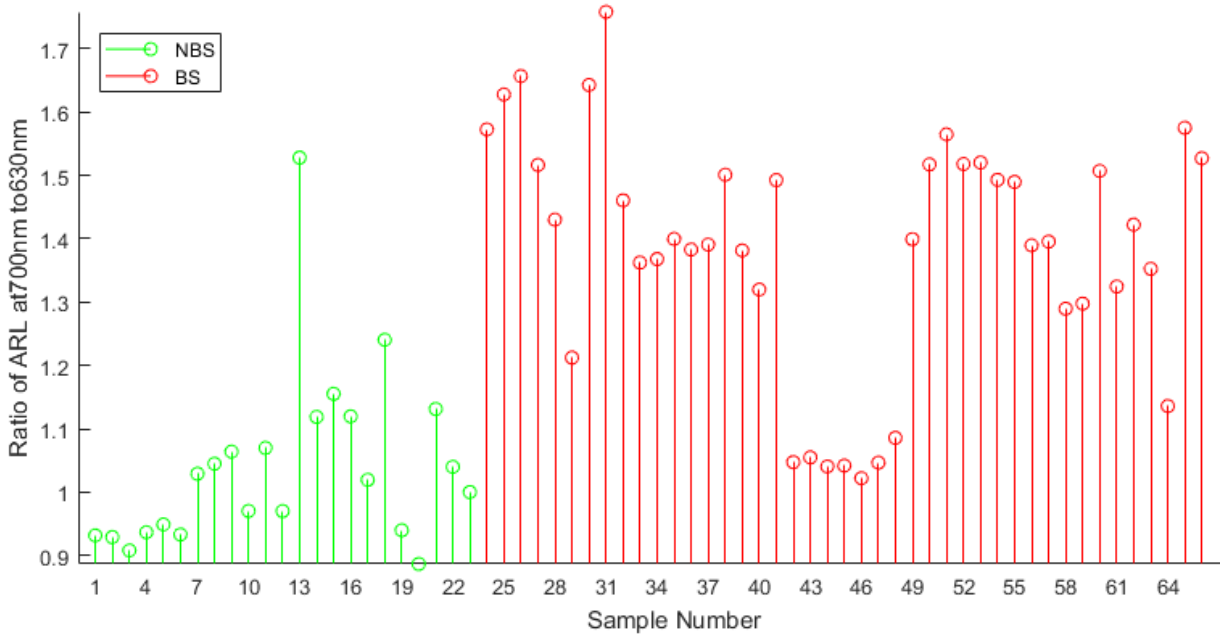

Figure 4-11: The ratio at (700 nm, 630 nm) for the second data set

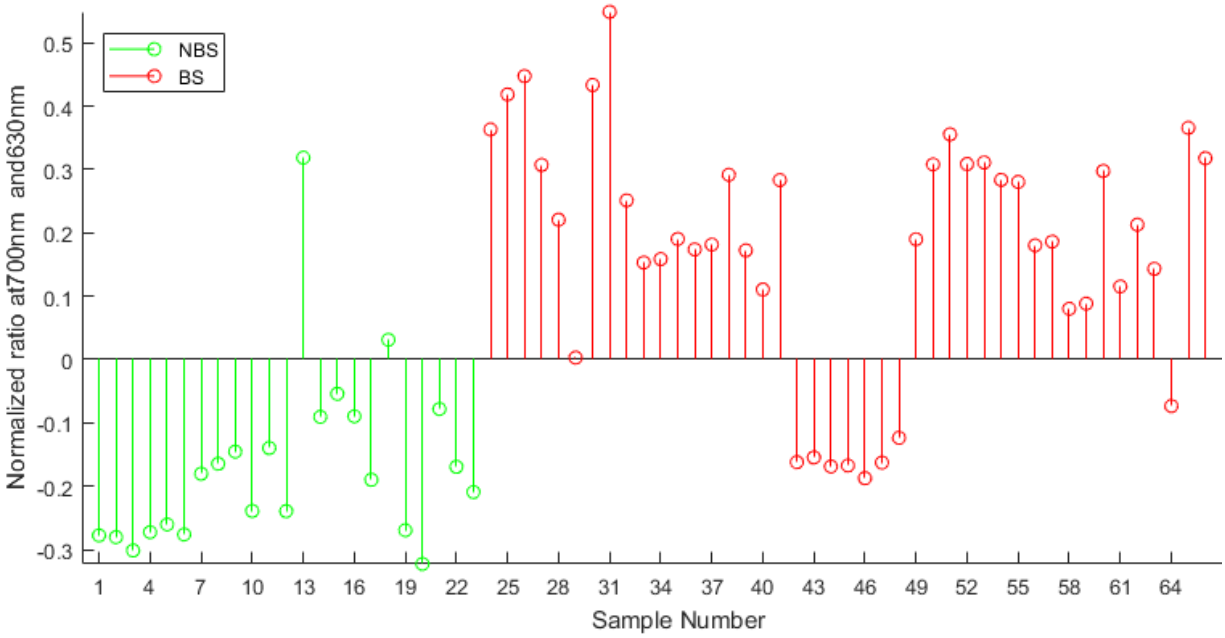

Figure 4-12: The normalized ratio at (700 nm, 630 nm) for the second dataset

This dataset includes a large number of samples which had more variations than that of the first dataset. Hence, the number of samples that may not be separate correctly would be more than that of the first dataset. For example, in Figure 4-12, the sample 13 (milk with chocolate syrup), and 18(the chopped orange pill with water) show a higher value than the cut-off point, and these samples are in the range of blood samples. Few blood samples (sample 42 to sample 48) also show a lower value than the cut-off point, and these samples are in the range of non-blood samples. These samples are the swine blood samples with the lower concentration (0.04% to 6.0%). The sample 64, horse blood sample with 25% concentration could be considered in mid-range concentration. Sample 29 is the hemoglobin solutions with a concentration of 18g/L, which could be treated as lower concentration, is also close to the separating line

The ratio at (480 nm, 530 nm) showed better performance for the second dataset than for the first dataset. Figure 4-13 and Figure 4-14 show the ratio at *(480 nm, 530 nm)* and the normalized ratio at *(480 nm, 530 nm)* where the cut-off point is found as 0.9189.

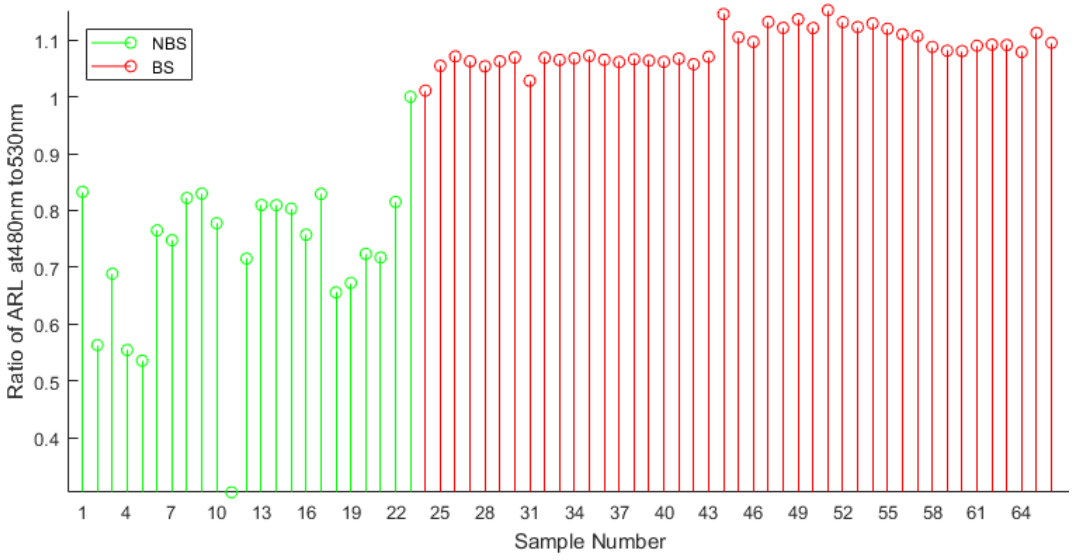

Figure 4-13: The ratio at (480 nm, 530 nm) for the Second data set

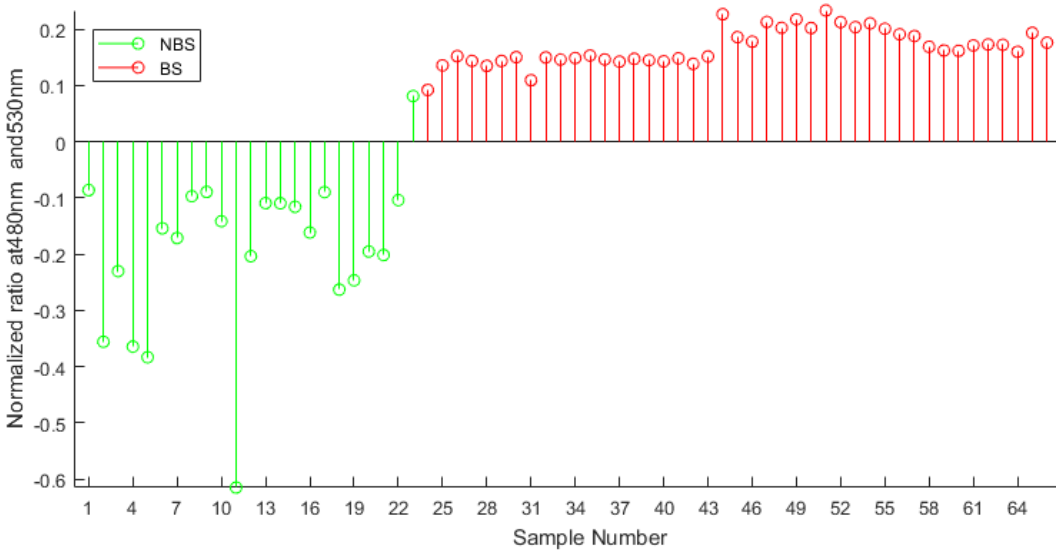

Figure 4-14: The normalized ratio at (480 nm, 530 nm) for the second dataset

The ratio and the normalized ratio at (480 nm, 530 nm) demonstrate an excellent separation. Most of the samples are separated properly other than sample 23 (water).

4.4 Results

In this analysis, two different datasets were used to investigate the spectrum of light which could be used to separate blood samples and nonblood samples. The ratio of ARL at two different wavelengths was calculated for each sample. A cut-off point (CP) of the ratio was determined to separate the blood samples from non-blood samples. The conditions for a sample "*i*" to be blood or non-blood sample could be written as

Blood samples: $ratio(i) >= CP$

Non- blood samples: $ratio(i) < CP$

The ratio at (700 nm, 630 nm) and the ratio at (480 nm, 530 nm) show better separation for both dataset. For the first datasets, while separating the samples using ratio at (700 nm, 630 nm),

the cut-off point was determined as 1.3664 which means that if the ratio is 1.3664 than the sample is highly likely to be a blood sample, and if less than that value then the sample should be a non-blood sample. For the second dataset, the cut-off point using the ratio at (700 nm, 630 nm) was found as 1.2093 which is very close to the cut-off point found in the analysis of the first dataset. As the cut-off points of both datasets are very close, it can be concluded that the proposed method is valid. The cut-off point found for the ratio at (480 nm, 530 nm) are also very close for both datasets. The values the cut-off points are shown in Table 4-1

Table 4-1: The value of the separating point at different pairs of wavelengths

Pair of wavelengths	**First dataset**	**Second dataset**
(700 nm, 630 nm)	1.3664	1.2093
(480 nm, 530 nm)	1.0095	0.9189

The number of total actual blood samples, non-blood sample, and detection of the samples by the algorithm is shown in the following tables. Table 4-2 shows the parameters of the first dataset for the ratio at (700 nm, 630 nm).

Table 4-2: Actual and detected states of the first dataset at (700 nm, 630 nm)

	Actual Blood Sample	**Actual Non-Blood Sample**
Detected as Blood Sample	22	0
Detected as Non-Blood Sample	0	13

Table 4-3 shows the parameters of the first dataset for the ratio at (480 nm, 530 nm). Table 4-4 shows the parameters of the second dataset for the ratio at (700 nm, 630 nm). Table 4-5 shows the parameters of the second dataset for the ratio at (480 nm, 530 nm). The accuracy of the algorithm for the datasets at different pairs of wavelengths are shown in Table 4-6.

Table 4-3: Actual and detected states of the first dataset at (480 nm, 530 nm)

	Actual Blood Sample	**Actual Non-Blood Sample**
Detected as Blood Sample	22	0
Detected as Non-Blood Sample	0	13

Table 4-4: Actual and detected states of the second dataset at (700 nm, 630 nm)

	Actual Blood Sample	**Actual Non-Blood Sample**
Detected as Blood Sample	35	2
Detected as Non-Blood Sample	8	21

Table 4-5: Actual and detected states of the second dataset at (480 nm, 530 nm)

	Actual Blood Sample	**Actual Non-Blood Sample**
Detected as Blood Sample	43	1
Detected as Non-Blood Sample	0	22

Table 4-6: Accuracy of the algorithm at different pairs of wavelengths

	First Dataset	**Second Dataset**
(700 nm, 630 nm)	100%	84%
(480 nm, 530 nm)	100%	98.48%

In this analysis, to maximize the accuracy of the proposed algorithm is not the objective, rather to find out region of operation where the samples could be separated properly. For the first dataset, all the samples were correctly identified by the algorithm. For the second dataset, the ratio at (480 nm, 530 nm) shows better performance than the ratio at (700 nm, 630 nm)

A comparison of Figure 4-12 with Table 3-2 shows that the blood samples which are not identified properly are mainly with low dilution samples.

4.5 Conclusion

Both ratios at 700 nm to 630 nm and 480 nm to 530 nm provide better separation. It should not be assumed that the ratio of ARL only at these two pairs of wavelengths will provide the separation, rather the separation at different other pairs of wavelengths around the suggested two pairs should also be considered as can be observed in Figure 4-6. This preliminary study provides a guideline for further study to detect gastrointestinal bleeding using the sensor. As the size of the spectrophotometer is huge compared to that of capsule endoscopy, spectrophotometer itself could not be used for capsule endoscopic procedure. Instead of using a spectrophotometer, two LED could be used whose wavelengths are same the suggested wavelengths in this study.

Chapter 5 Analysis with Infrared and Red Light

It was shown in the previous chapter that both pairs of (700 nm, 630 nm) and (480 nm, 530 nm) are important to separate BS and NBS. This chapter describes the outcome of the analysis with infrared (IR) and red(R) light. The infrared light falls in a different region of the optical spectrum than the spectrum used in the previous experiment. The objective of this part of the study is to separate of BS and NBS with respect to infrared and red light. Some of the previous researchers used the red light and violet light and they were able to distinguish BS and NBS to some extent[64]–[66]. For simplicity of hardware, a pulse oximeter sensor is used for this analysis in which both IR and red light source and receiver are integrated. This chapter will first discuss the working principle of the pulse oximeter, procedure of data collection and interface with the microcontroller and computer. Then, analysis of the first dataset is presented. The same datasets as described in the previous experiment were used in this experiment. The first dataset is used to find the optical characteristics of BS and NBS by which the samples could be separated with respect to IR and red light. Validation of the analysis with the second dataset is presented finally.

5.1 Pulse Oximeter Sensor

A pulse oximeter is mainly used to determine the oxygen saturation of blood in a non-invasive way. It emits red light and infrared light sequentially from one side through finger and measures the amount of transmitted light from another side. These measurands are used to determine the percentage of hemoglobin that is bonded with oxygen. However, these measurands could also be used to distinguish blood samples and non-blood samples. A commercial Pulse oximeter sensor is shown in Figure 5-1 [77].

Figure 5-1: Commercial pulse oximeter sensor used in the experiment

5.1.1 Working Principle

The pulse oximeter sensor has both infrared and red LED connected back to back. These lights can be controlled by only two pins of any microcontroller. At the end, the device is connected to a DB9 connector which has 09 pins. While pin 2 is high and pin 3 is low, infrared LED is activated and when the status of these pins are reversed red LED is activated. The transmitted light activates the photodiode which is connected to pin 5. The photodiode creates voltage according to the intensity of transmitted IR light and red light. The voltage is measured by the microcontroller. Pulse oximeter pinout with DB9 connector is shown in Figure 5-2 [78]. The experiment setup with Pulse sensor is shown in Figure 5-3.

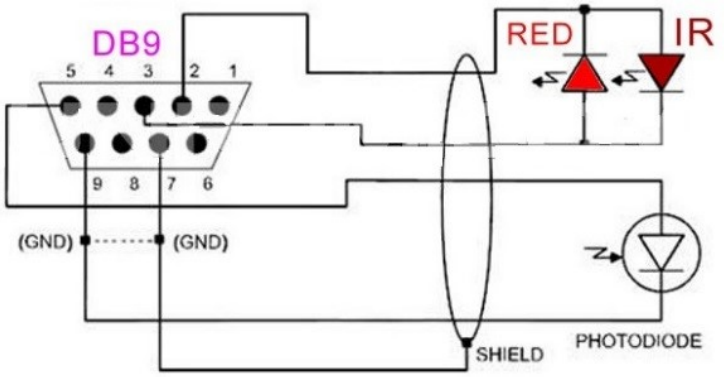

Figure 5-2: Pulse oximeter pinout with DB9 connector

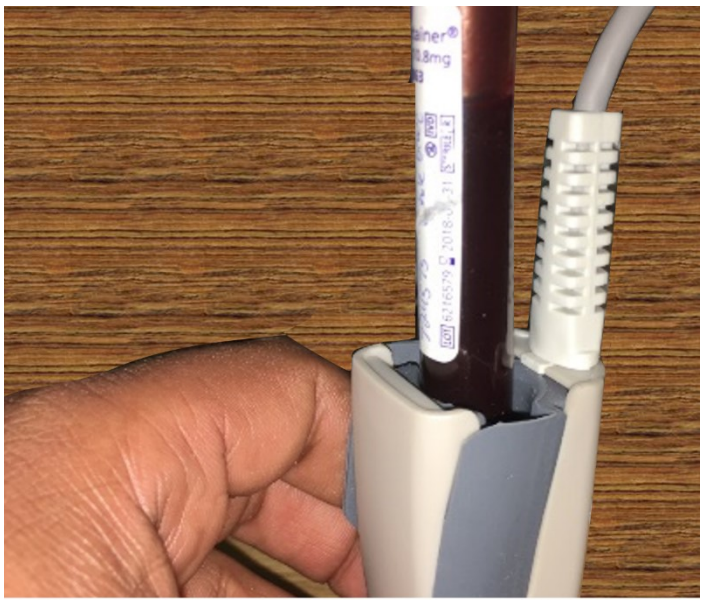

Figure 5-3: Pulse oximeter sensor and experiment with samples

5.1.2 Procedure of Data Collections

A microcontroller, Arduino Uno was connected to the pulse oximeter. Two digital outputs (pin15, and pin 16) of the microcontroller were connected to two pins of the DB9 connector (pin 2 and pin 3). One analog input (pin 14) read the value of transmitted light as the corresponding voltage level. Also, the microcontroller was programmed to read IR value only when IR LED was

active and red value only when the red LED was active. The connection between pulse oximeter and Arduino Uno is shown Table 5-1. The whole experimental setup was connected to a computer where MATLAB interface was used to receive the data transmitted by Arduino Uno.

Table 5-1: Connection between pulse oximeter and Arduino Uno

	DB9 of pulse oximeter sensor	Arduino Uno
Red LED	3	15
IR LED	2	16
Analog Reading	5	14
GND	GND	GND

The sensor was fixed in a certain position so that the effects due to the motion artifacts were reduced. The collected data was saved in Microsoft Excel file. For each of the samples, the mean of 100 reading was used in the analysis. The reading of the first dataset and the second dataset were taken at a different date. It was possible that the ambient light, temperature and few other factors were in a certain state for the first dataset and in another state for the second dataset. Although the states were supposed to be same for both dataset, there might be small differences between the two states. However, the difference should cancel out by using filters and other electronic optimizers. For standard devices, all necessary components are integrated with the device so that effects of the states are nullified, and performance remains same for different states. As the system designed by using the pulse oximeter in this experiment was not a standard system, it was a better idea to remove those effects. To do that, the readings of all samples were normalized based on the reading of water, for example, reading of a sample divided by the reading of water.

5.2 Analysis of the First Dataset with Pulse Oximeter Sensor

The response of a sample has two value such as IR and red. Hence, the response of any sample *n* could be defined as:

Response(n)=F(IR, red)---------- (5-1)

As the reading of each sample was normalized based on the response of water. The response of a sample could be written as:

Response(n)= Response(n)/ Response(water) ----------(5-2)

Equation (5-2) has two value, IR and red (R).

IR_Response(n)= IR_Response(n)/ IR_Response(water) ----------(5-3)

R_Response(n)= R_Response(n)/ R_Response(water) ----------(5-4)

For water, both IR and R responses are 100%. Figure 5-4 shows the normalized intensity of transmitted red light vs that of transmitted infrared light. Figure 5-4, it is clear that the blood samples (BS) are almost in the same region whereas the non-blood solutions are in a different region. The region for the presence of blood could be noticeably identified from this figure. Red circles show the blood samples and the green triangles show the non-blood samples (NBS) in this figure.

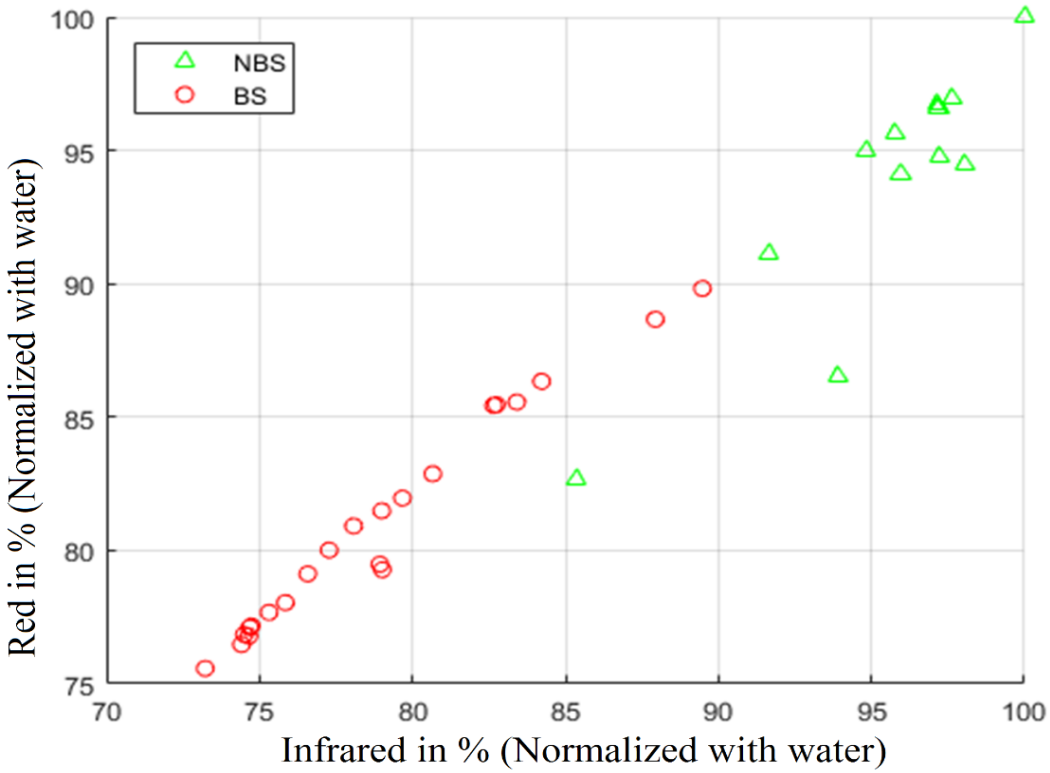

Figure 5-4: Normalized value of red channel vs infrared channel of the first dataset

5.2.1 Development of the Algorithm

Few of the previous researcher used the ratio of red light and violet light to investigate the differences in characteristics of BS and NBS [64]–[66]. Here, the ratio of the amount of transmitted light (ATL) of the red spectrum to that of the infrared spectrum was used to separate the samples. This ratio provides a clear distinguishable parameter to separate each type of samples. The ratio for a sample *i* could be expressed by the following function:

$$Ratio(i) = \frac{R\_Response(i)}{IR\_Response(i)} \text{ ----------(5-5)}$$

A cut-off point was found above which the samples were identified as BS and below which the samples were identified as NBS. The ratio was normalized by subtracting the cut-off point (CP) from the ratio.

$$Normalized\ Ratio(i) = \frac{R(i)}{IR(i)} - CP \text{ ----------(5-6)}$$

Where CP was calculated by taking the mean of the median of BS and median of NBS. From now on for this chapter, the term "ratio" will mean the ratio of the amount of transmitted red light to that of infrared light. The term "normalized ratio" will mean the ratio after subtracting the cut-off point.

5.2.2 Performance of the Algorithm on the First Dataset

Figure 5-5 and Figure 5-6 respectively. The cut-off point for this dataset was found as 101.1743 which signifies that if the ratio is more than 101.1743, the samples are highly likely to be a blood sample, and if the ratio is less than that, the sample should be a non-blood sample.

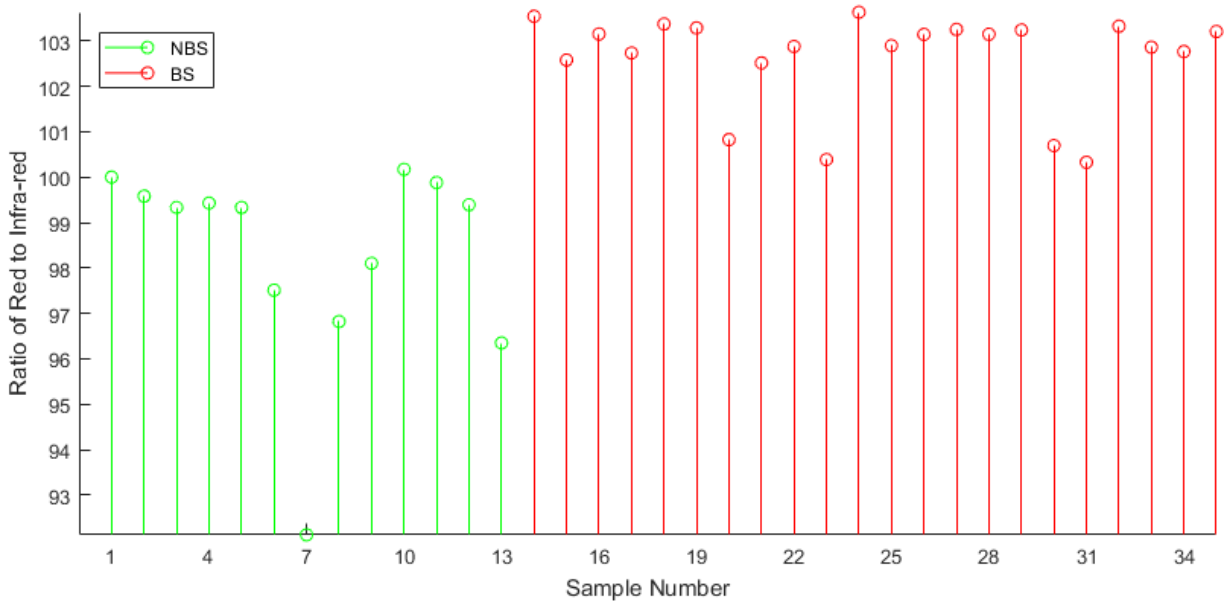

Figure 5-5: The ratio for the first dataset

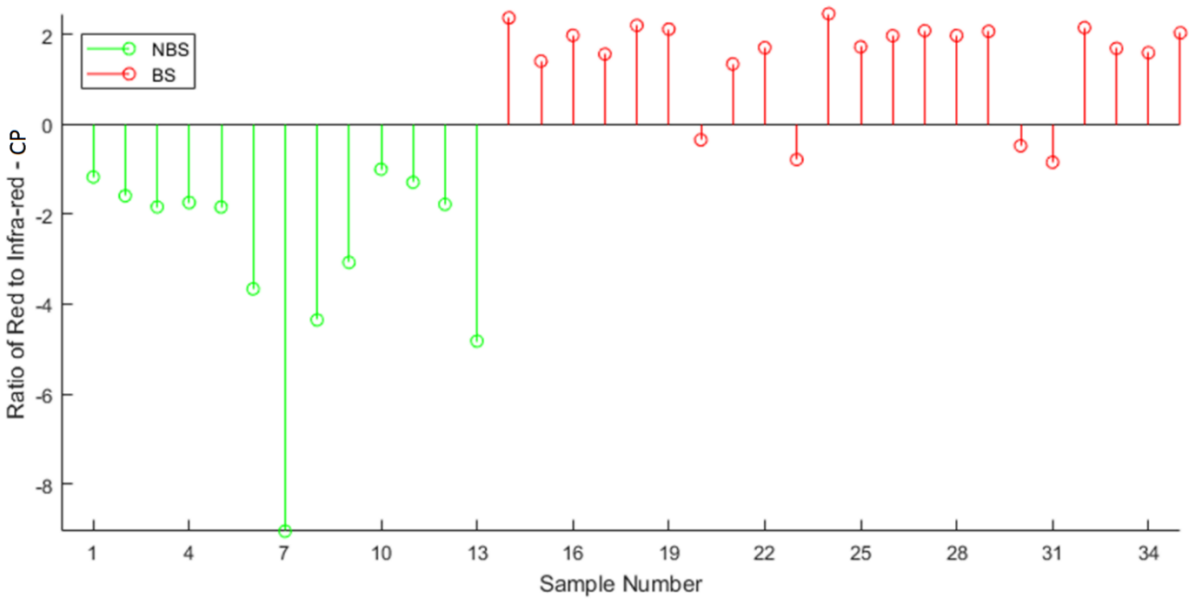

Figure 5-6: Normalized ratio for the first dataset

The above figures show that some blood samples such as samples 20, 23, 30 and 31 are identified as non-blood samples by this algorithm. Sample 20 is horse blood sample with 8% concentration, sample 23 is swine blood (6%), and sample 30 and 31 are hemoglobin solutions with 19.4 g/L and 22.8g/L concentration. The samples are mainly low concentration of blood and hemoglobin samples. Hence, for the first dataset, the proposed algorithm fails to identify low concentration blood samples properly. The performance could be checked by using the second dataset.

5.3 Validation of Analysis with the Second Dataset

A different dataset was used here to validate the theory which was developed in the previous section. With same hardware configuration and almost similar environment, 43 blood samples and 23 non-blood samples were used for this dataset. Normalized value of red channel vs infrared channel is shown in Figure 5-7.

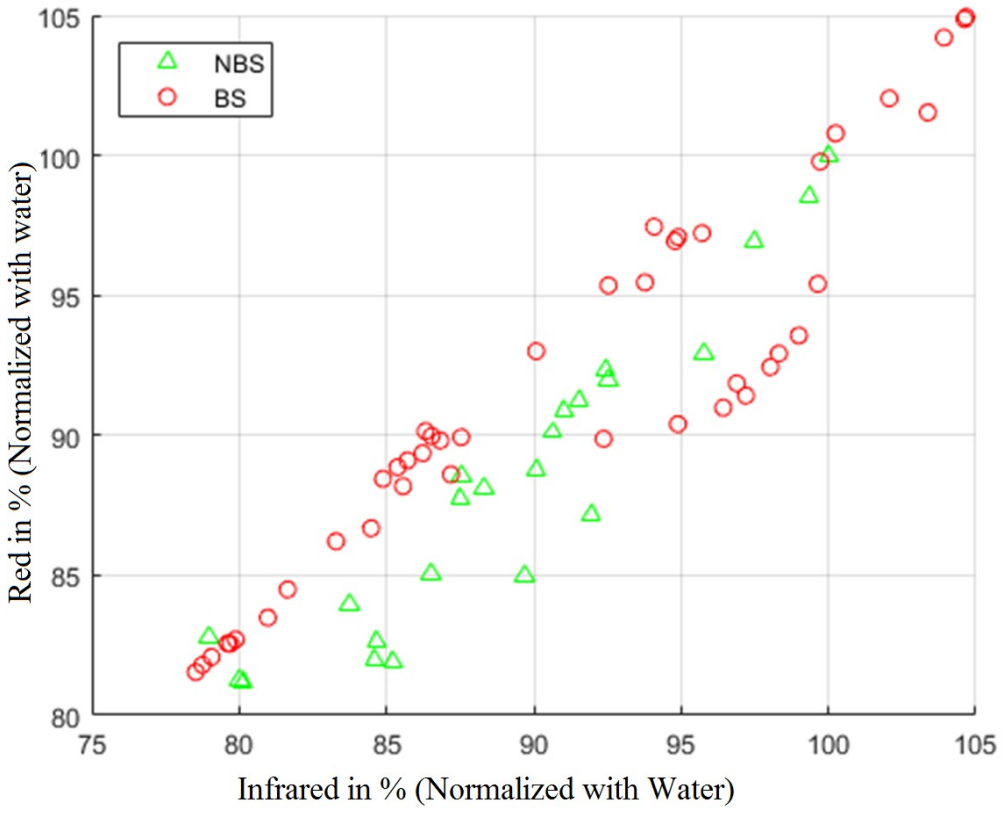

Figure 5-7: Normalized value of red channel vs infrared channel of the second dataset

The pattern shown for the second dataset in Figure 5-7 looks different than pattern shown for the first dataset in Figure 5-3. Few of the samples are fall in the region of non-blood samples which can be observed clearly in this figure. The ratio and the normalized ratio for the second dataset is shown in Figure 5-8 and Figure 5-9 respectively. The cut-off point was found as 101.0062 in this case.

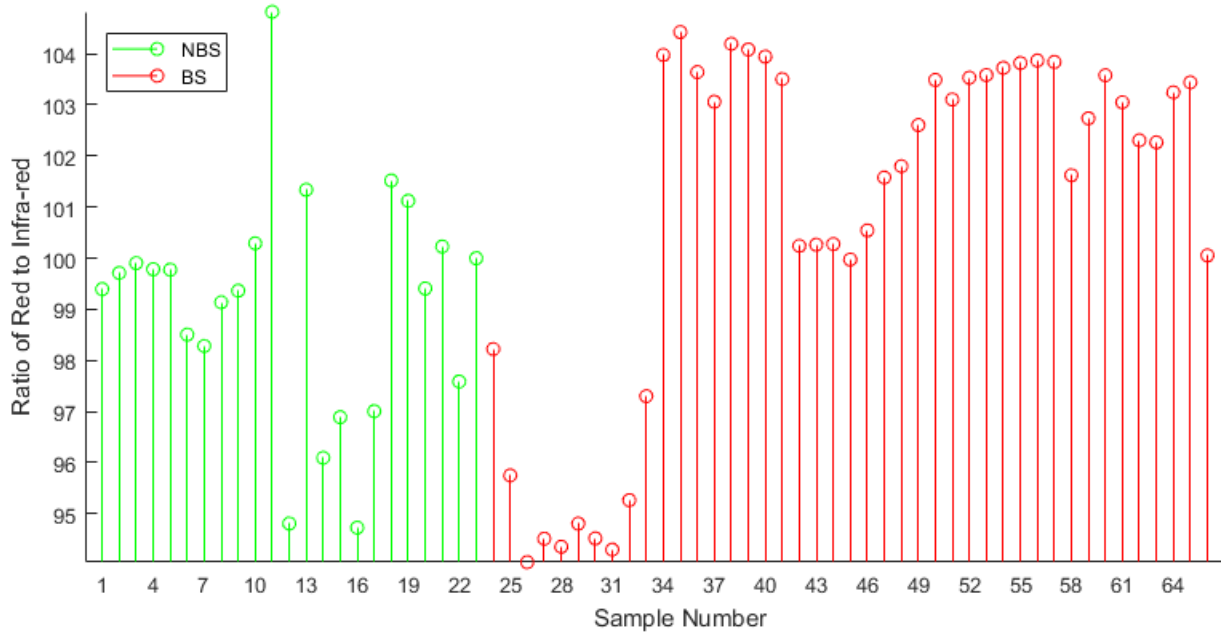

Figure 5-8: The ratio for the second dataset

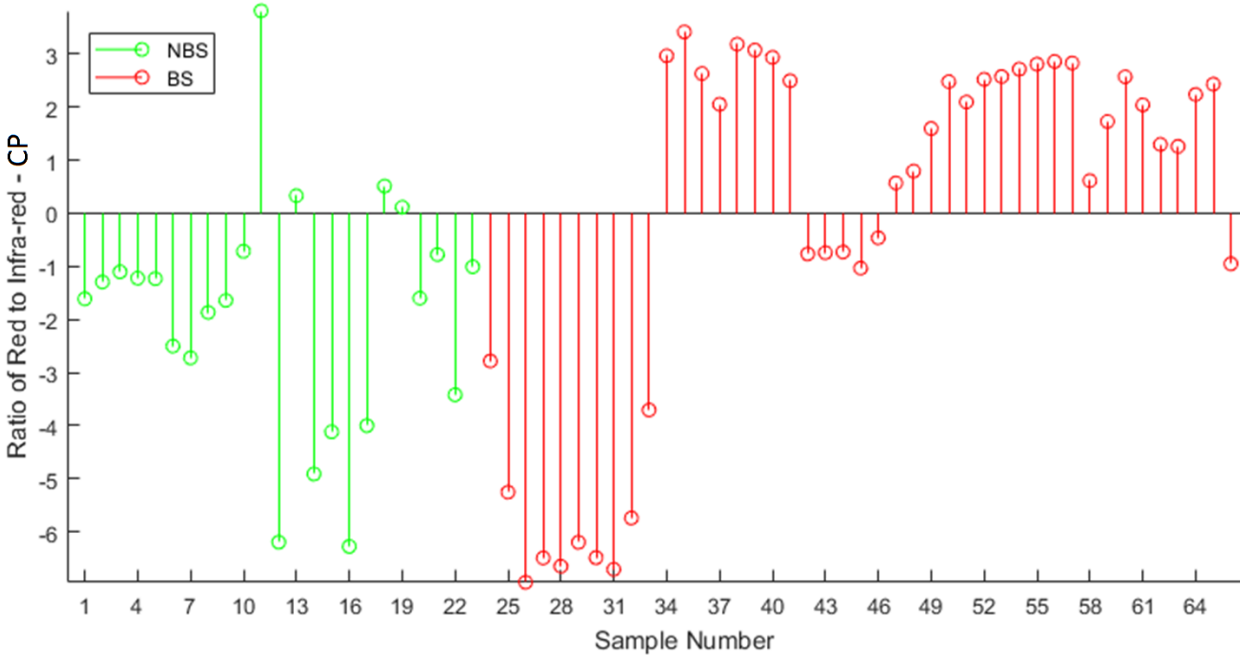

Figure 5-9: The normalized ratio for the second dataset

The non-blood samples which fall in the region of blood samples are 11,13,18,19. These samples are milk with yogurt and turmeric powder (11), milk with chocolate syrup (13), chopped

orange pill with water cashed vitamin C tablet (19). On the other hand, sample 24 to 33, 42 to 46 and 66 which are blood samples, fall in the region of non-blood samples. Samples 24 to 33 are the hemoglobin solutions with a lower concentration (3g/L to 20gm/L), samples 42 to 46 are the swine blood samples with a lower concentration (0.04% to 2.0%), and sample 66 is a horse blood sample with a concentration of 4%.

Application of the algorithm on both datasets shows that separation between BS and NBS is possible by using the ratio of ARL of infrared light to that of red light. However, in both case, the proposed algorithm fails to detect the lower concentration of blood solution. Details performance could be found by comparing Figure 5-6 with Table 3-1, and Figure 5-9 with Table 3-2.

5.4 Results

In this experiment, the ratio of ATL of the red spectrum to that of the infrared spectrum was used to distinguish the blood samples from non-blood samples. A cut-off point was determined to draw the separating line between the samples. A sample "i'' could be separated using the cut-off point *(CP)* based on the following conditions.

Blood samples: *ratio(i) >=CP*

*N*on- blood samples: *ratio(i) <CP*

Table 5-2: Actual state and detected state of the samples for the first dataset

	Actual Blood Sample	**Actual Non-Blood Sample**
Detected as Blood Sample	18	0
Detected as Non-Blood Sample	4	13

The number of total blood samples, non-blood samples, and detection of the samples by the algorithm is shown in the following tables. Table 5-2 shows the parameters of the first dataset and Table 5-3 shows the parameters of the second dataset. The accuracy of the algorithm for the datasets is shown in Table 5-4.

Table 5-3: Actual state and detected state of the samples for the second dataset

	Actual Blood Sample	**Actual Non-Blood Sample**
Detected as Blood Sample	27	4
Detected as Non-Blood Sample	16	19

Table 5-4: Accuracy of the algorithm

First Dataset	**Second Dataset**
88.57%	69.70%

5.5 Conclusion

The objective of this analysis was to explore a parameter using a pulse oximeter to differentiate the blood samples from the non-blood samples. Most of the samples were identified using the ratio of red light to infrared light (equation 5-2) properly. For both datasets, it was explored that if the ratio is more than the cut-off point, the samples are more likely to be a blood sample, and if less than the cut-off point, the samples are more likely to be a non-blood sample. The remarkable fact is that the cut-off points (101 as a round figure) for both datasets are found very close. However, as the ratio of some of the BS and NBS are near to each other, those samples should be reevaluated. Few blood samples with low concentration were not properly detected using the proposed ratio. The next chapter will discuss the analysis of the same datasets using the RGB colour sensor.

Chapter 6 Analysis with RGB Sensor

The ratio of the amount of transmitted infrared light to red light provides a distinguishable feature to separate the blood samples and non-blood samples which are described in the last chapter. Analysis of the samples using the RGB colour sensor will be discussed in this chapter. Any colour can be expressed as a combination of red, green and blue colour. The RGB colour sensor provides the colour information of an object through three different analog channels. The function of these values could be used to separate the BS and NBS. The objective of this part of the study is to explore the relationships among these values where the separation will be maximum. The RGB colour sensor, its working principle and the interface with Arduino Uno and computer are discussed first and then the analysis of the first dataset is presented. Finally, the performance of the developed algorithm is presented using the second dataset.

6.1 RGB Colour Sensor

The RGB colour sensor (HDJD S-822) is a simple optical sensor. It works similar way to the spectrophotometer. However, it emits white light and converts the reflected RGB light into the corresponding analog voltage output. The reflected light from an object received by three different photodiodes red (R), green (G) and blue (b). The outputs of these photodiodes are available to read through three different analog channels and output voltage range of the channels are from 0v to 3v. Analog voltages of the channels are measured by a microcontroller, Arduino Uno. The output of the channels should be calibrated according to the datasheet provided by the manufacturer[79]. The calibration is done within microcontroller program. The received data can be shown on Arduino platform. To save the data in Microsoft Excel file, an appropriate interface should be used to communicate with the Arduino. The front and back side of this sensor are shown in Figure 6-1.

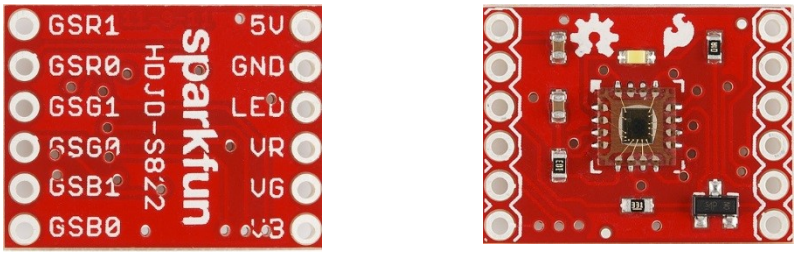

Figure 6-1: Back side and front side of RGB sensor

6.1.1 Working Principle

The RGB sensor was connected to an Arduino Uno microcontroller. The feedback registers used to select the channel gain were used as 3.00M Ω. This was done by grounding all the gain selection pins, GSR1, GSR0, GSG1, GSG0, GSB1, GSB0. The white LED was controlled by using a digital output (pin 14) from the Arduino Uno microcontroller. The outputs of the red channel, green channel and blue channel of the RGB colour sensor were measured by three different analog inputs A1, A2 and A3 pins of the Arduino Uno microcontroller. Ground pin and 5V pin of the sensor and the microcontroller were also connected to each other. The connection diagram of the sensor with Arduino Uno is shown in Figure 6-2 which is shown in a tabular form in Table 6-1.

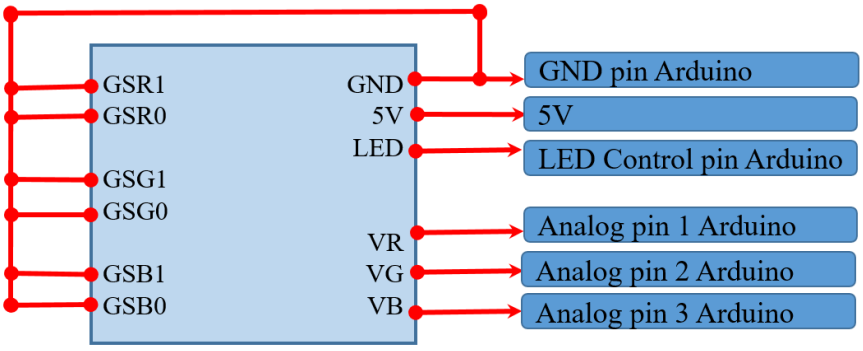

Figure 6-2: Block diagram of RGB sensor interface with Arduino Uno

Table 6-1: Connection between RGB sensor and Arduino Uno

RGB Sensor	Arduino Uno	Description
5V	5V	Power Supply
GND	GND	GND
LED	14	Turn on the white LED
VR	A1	Read the value at red Channel
VG	A2	Read the value at green Channel
VB	A3	Read the value at blue Channel
GSR0, GSG0, GSB0 GSR1, GSG1, GSB1	GND	Channel Gain

6.1.2 Data Collection

The RGB sensor was connected to the microcontroller according to Figure 6-2. The microcontroller was connected to a computer via USB port. Although the RGB colour sensor is a finished product, application of RGB sensor to separate the blood from non-blood samples is not a standard system. A cuboid black box was used to minimize the external interface and the motion artifacts. Arduino measured the readings and sent those readings to a computer which was received in MATLAB. The mean of 100 reading was used in the analysis for each sample. The datasets were normalized based on the value of water by the same way done in case of the pulse oximeter sensor to cancel out the effect of different conditions of different datasets. Experiment setup with the RGB sensor is shown in Figure 6-3. There was a small square shaped basement that helped the test tube to stay in a fixed position while taking the measurement. The sensor was also properly fixed so that it had the same distance from the test tube for all the samples.

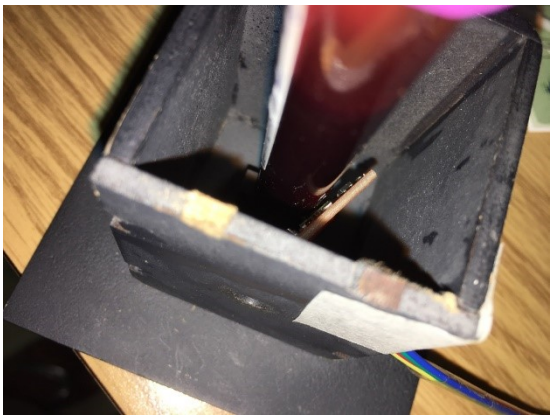

Figure 6-3: Experimental setup using RGB sensor

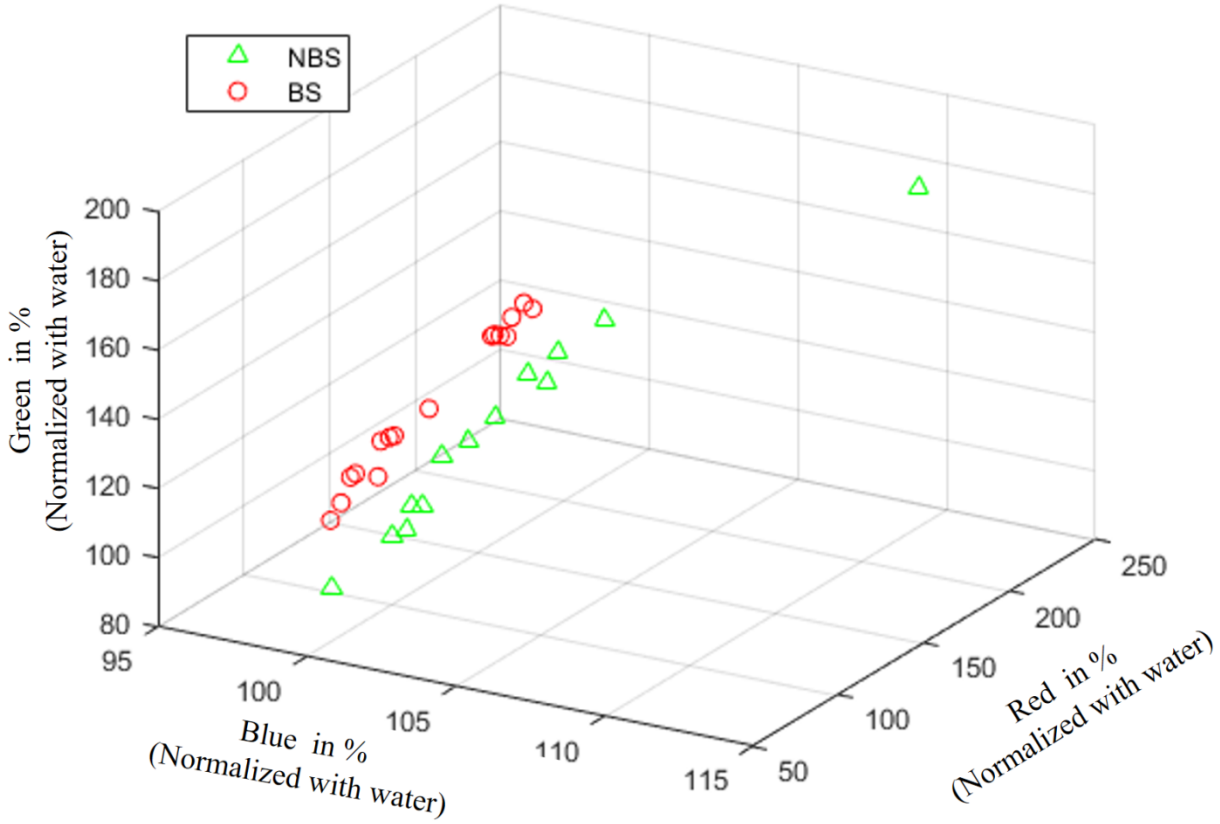

Figure 6-4: Blood Samples and other Samples are in Different Region

6.2 Analysis of the First Dataset

The received data were saved in Microsoft Excel file. The microcontroller sent the reading in order of blue, red and green channel value. The complete dataset was normalized by dividing each of blue, red and green channel value of a sample by corresponding value of water. Hence, the values of water are 100% for each of the three channels. The normalized values for each of the samples are plotted in Figure 6-4.

In Figure 6-4, it can be clearly observed that both BS and NBS are in a different region. Also, BS and NBS are following a different pattern. The dataset was further processed by subtracting the mean value of each channel from that channel. The first thing to determine the separation between the samples was to use the ratio of each two channels. However, the results were not satisfactory. Instead of using ratio, a line of separation in a two-dimensional plane was used here.

6.2.1 Development of the Algorithm

Few of the previous researcher used some derived parameters using the values of red, green and blue channel values [42], [69]. In the first part of this study, the ratio of the intensity of reflected light at two different wavelengths was used in the analysis performed by the spectrophotometer. Further, the ratio of the red light and violet light was used in case of the pulse oximeter. In case of the RGB sensor, the ratio and few other derived forms were analyzed to investigate the differences between the characteristics of BS and NBS. However, one of the derived parameters that had better performance is discussed in this chapter. Figure 6-4 illustrates that the blood samples and non-blood samples are following different lines. For simplicity and to reduce the number of components that might be integrated with the capsule endoscopy, two-dimensional

analyses were performed here. Among blue, red and green, only two channels were analyzed at a time. A function to separate the samples, *FS,* was defined using only two channels of the three. This function can be expressed by the following equation:

$FS_i(X,Y) = Y(i) - m * X(i)$----------(6-1)

Where *X and Y* are any two channels of RGB sensor, *i* is the sample number, and *m* is a constant found by the following operations:

1. Finding gross sloop (m_1) of a line that fit for the blood samples
2. Finding gross sloop (m_2)of a line that fit for the non-blood samples
3. Finding *M,* the average of m_1 and m_2
4. Finding the separation by using equation (6-1) for *M.*
5. Searching a better separation by using few more value of the sloop around *M*.
6. Selecting the value of *M* as *m* where equation (6-1) provides maximum accuracy.

For example, if *X* and *Y* represent the red and blue channel, the equation (6-1) will be

$FS_i(Red, Blue) = Blue(i) - m * Red(i)$----------(6-2)

The function $FS_i(X, Y)$ is actually the intersection point of a line with a sloop of *m.* From now on, the term "*intersection(X, Y)* " will mean the point of intersection of a line on *Y-axis.* The optimum sloop of the line *m* is determined by using the steps above.

6.2.2 Performance of the Algorithm on the First Dataset

Here results for the *intersection (Blue, Red), intersection (Green, Red),* and *intersection (Blue, Green)* are shown in Figure 6-5 to Figure 6-7, for the corresponding optimum value of *m*. The summary of the analysis is shown in Table 6-2

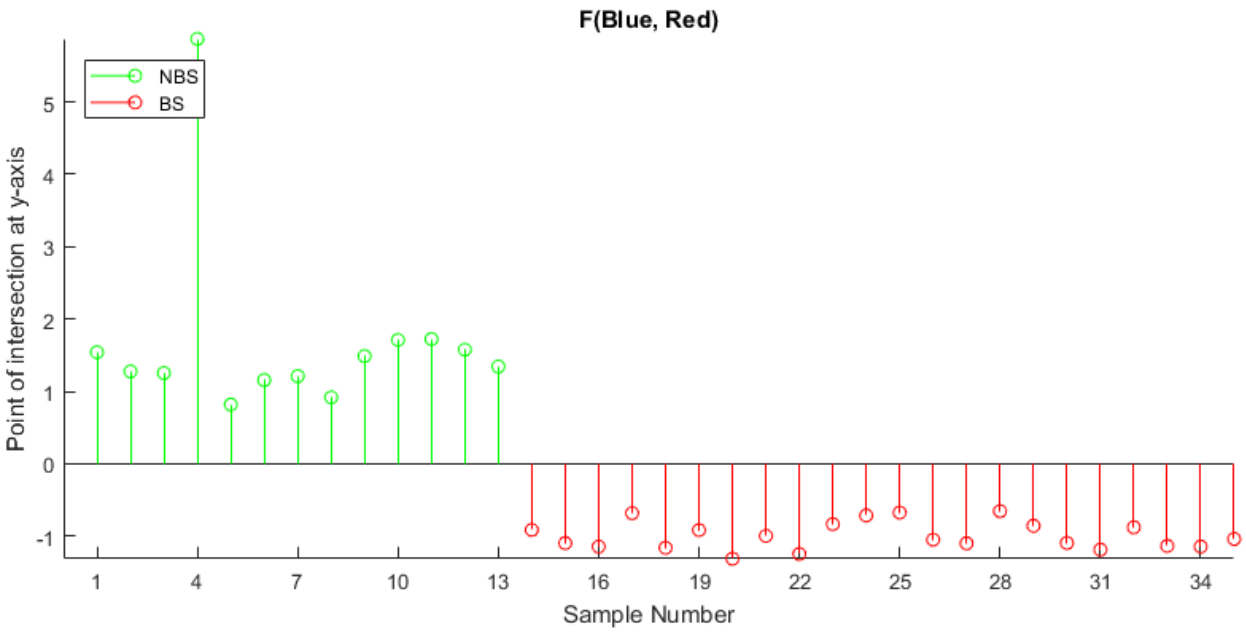

Figure 6-5: *Intersection (Blue, Red), m*= 0.0814, for the first dataset

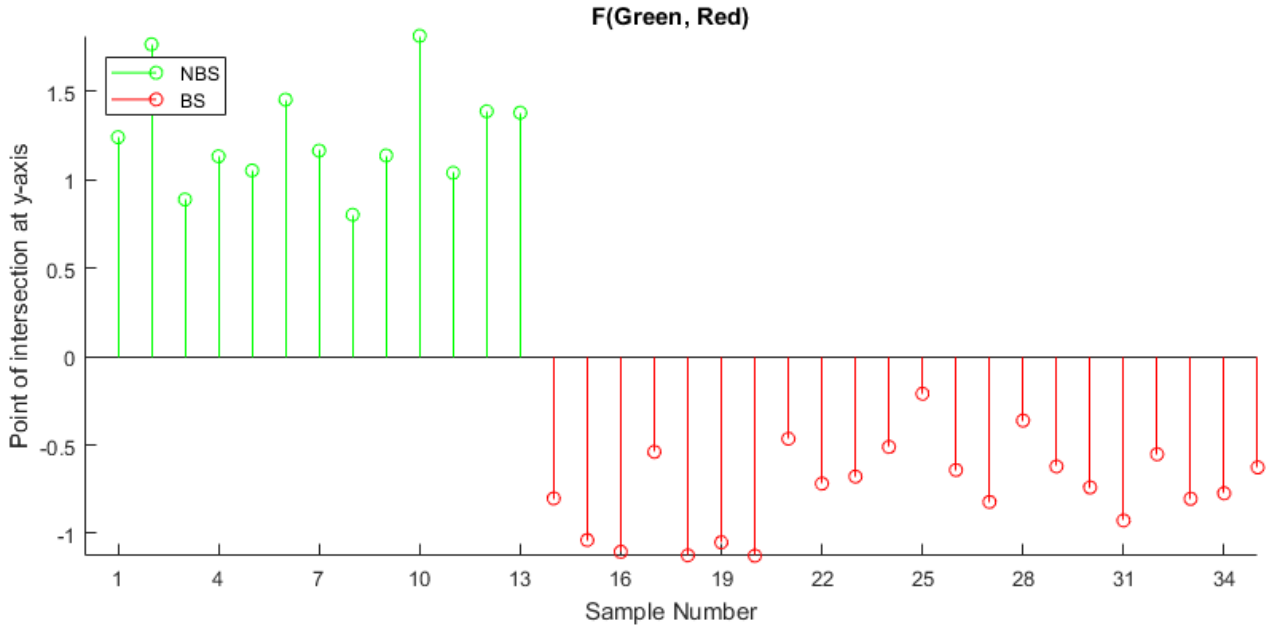

Figure 6-6: *Intersection (Green, Red), m*= 0.1083, for the first dataset

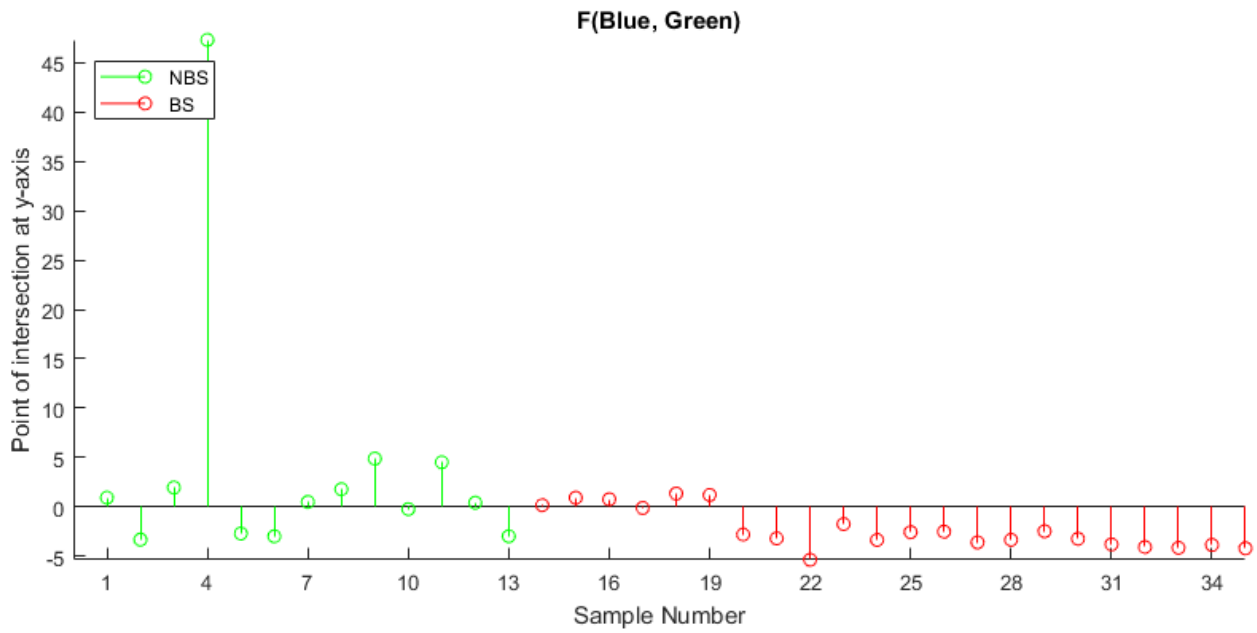

Figure 6-7: *Intersection(Blue,Green), m*= 0.6911, for the first dataset

Table 6-2: Optimum value of m and accuracy of separation for the first dataset

SL No	***x***	***y***	**Optimum value of m**	**Accuracy of Separation**
1	Blue	Red	0.0814	100%
2	Green	Red	0.1083	100%
3	Blue	Green	0.6911	71.42%

Figure 6-5 and Figure 6-6 show the *intersection (Blue, Red)* and *intersection (Green, Red)* where the separation is possible perfectly. For both cases, the value of the function is negative for the blood samples. However, the function *intersection (Blue, Green)* shown in Figure 6-7 does not show the separation properly. The performance could be validated using the second dataset.

6.3 Validation of Analysis with the Second Dataset

The same functions intersection(X, Y) with the corresponding value of m were used here to verify the proposed analysis. The analysis was applied to the second dataset. The results of the functions intersection (Blue, Red), intersection (Green, Red), and intersection (Blue, Green) are shown in Figure 6-8 to Figure 6-10. The summary of the analysis is shown in Table 6-3.

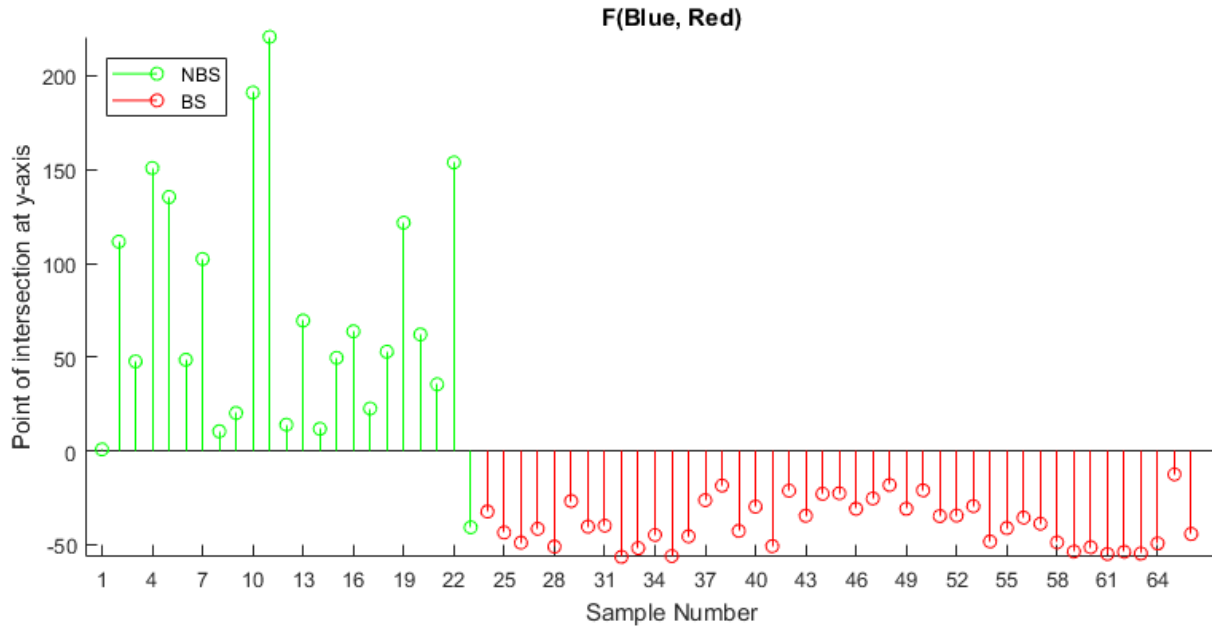

Figure 6-8: *Intersection (Blue, Red), m*=0.0814, for the second dataset

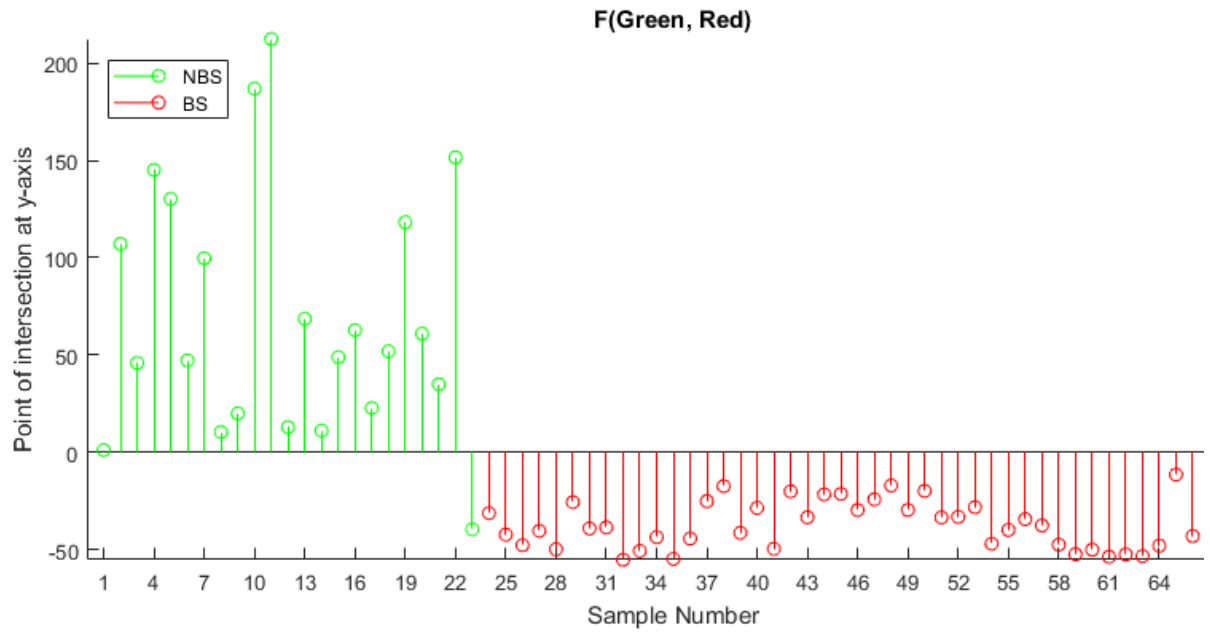

Figure 6-9: *Intersection(Green, Red), m*=0.1083*,* for the second dataset

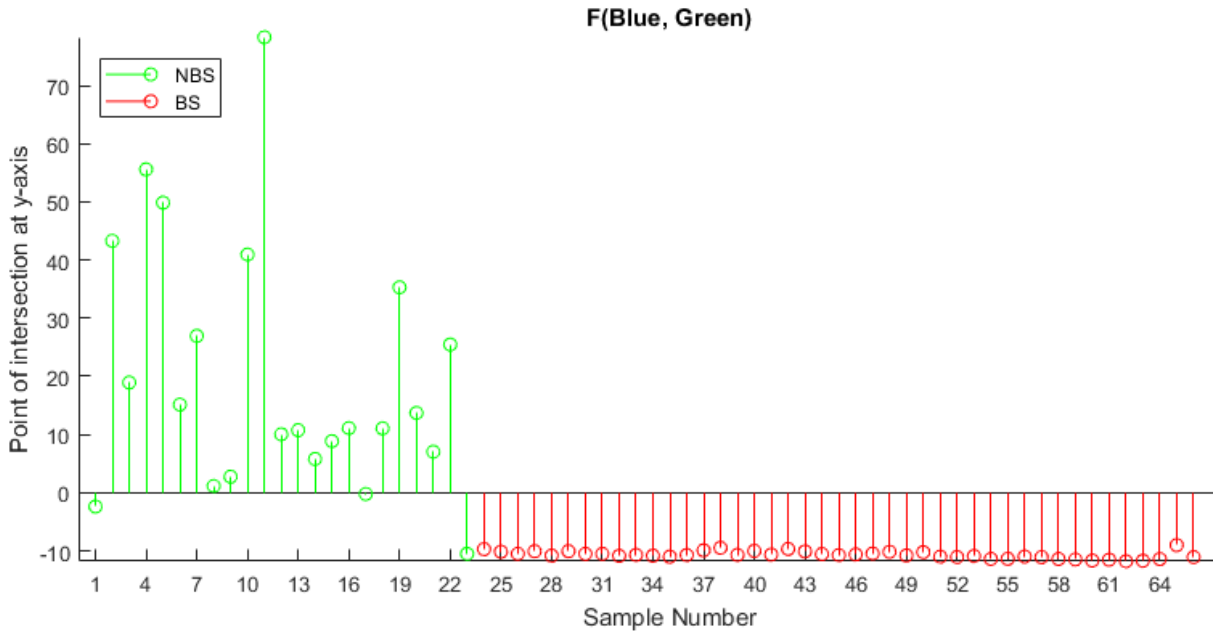

Figure 6-10: *Intersection(Blue, Green), m=0.6911,* for the second dataset

Table 6-3: Optimum value of m and accuracy of separation for the second dataset

SL No	*x*	*y*	Optimum value of m	Accuracy of Separation
1	Blue	Red	0.0814	98.48%
2	Green	Red	0.1083	98.48%
3	Blue	Green	0.6911	95.45%

All the three functions presented for the second dataset show very good result. However, sample 23 (water) falls in the region of BS. Other than this, most other samples show good separation. The positive value of the function indicates non-blood samples and the negative value indicates blood samples for both datasets. An important fact can be noticed that the range of the FS for the first dataset is different (around 10) than that for the second dataset (around 100).

6.4 Results

The RGB sensor reads the reflected light through three different analog channels such as red, green and blue channel. A combination of any two of the channels was used here to distinguish the blood samples from the non-blood samples. The channels were considered as the two variables of a linear equation and the intersection of the line at y-axis was considered as a parameter to separate the samples. However, no cut-off point was used here as used in the previous two analyses. The samples were separated by the zero line. Hence, the cut-off point could be said as zero. This is because the mean of each channel was subtracted at an earlier stage of this analysis. Hence, the conditions for a sample "*i*" to be a BS or NBS are:

Blood samples: $intersection(i) < 0$

Non- blood samples: $intersection\ (i) > 0$

Three different combinations of the channels were used in this analysis. The function *intersection(i)* was optimized based on a parameter, m, which has already been discussed in section

6.2. The number of actual and detected of the samples by the algorithm for the first dataset is shown in Table 6-4, Table 6-5, and Table 6-6 for the three combinations of the channels. The tables also show about the function *intersection* and *m*.

Table 6-4: Actual and detected states of the first dataset, function: *(Blue, Red), m*= 0.0814

	Actual blood sample	**Actual non-blood sample**
Detected as blood sample	22	0
Detected as non-blood sample	0	13

Table 6-5: Actual and detected states of the first dataset, function:*(Green, Red), m*= 0.1083

	Actual Blood Sample	**Actual Non-Blood Sample**
Detected as Blood Sample	22	0
Detected as Non-Blood Sample	0	13

Table 6-6: Actual and detected state of the first dataset, function:*(Blue, Green), m*= 0.6911

	Actual Blood Sample	**Actual Non-Blood Sample**
Detected as Blood Sample	17	8
Detected as Non-Blood Sample	5	5

The same parameters shown in Table 6-7, Table 6-8 and Table 6-9 for the second dataset including *intersection* and *m.*

Table 6-7: Actual and detected state of the second dataset, function: *(Blue, Red), m*=0.0814

	Actual Blood Sample	**Actual Non-Blood Sample**
Detected as Blood Sample	43	1
Detected as Non-Blood Sample	0	22

Table 6-8: Actual and detected state of the second dataset, function: *(Green, Red), m*=0.1083

	Actual Blood Sample	**Actual Non-Blood Sample**
Detected as Blood Sample	43	1
Detected as Non-Blood Sample	0	22

Table 6-9: Actual and detected state of the second dataset, function: *(Blue, Green), m=0.6911*

	Actual Blood Sample	**Actual Non-Blood Sample**
Detected as Blood Sample	43	3
Detected as Non-Blood Sample	0	20

6.5 Conclusion

The objective of this experiment was to explore the relationships among the channels of the RGB sensor so that the blood samples could be differentiated from non-blood samples. For both datasets, the performance of *Intersection (Blue, Red*) and *Intersection (Green, Red)* are better than that of *Intersection (Blue, Green)*. Hence red channel is important to distinguish the blood samples from the non-blood samples. These analyses could be used to detect the blood in the GI tract. The next chapter will summarize the findings and compare the performance of this word with few of the previous works.

Chapter 7 Summary and Comparison

The last three chapters described the analyses and the results of the samples using three different instruments such as the spectrophotometer, the pulse oximeter, and the RGB colour sensor. The instruments were used to explore the ways to separate the blood samples from the non-blood samples. The summary of the findings will be summarized in this chapter and then a comparison with some previous works will be presented here.

7.1 Summary

Analyses of the samples conducted by three different instruments suggest the possibilities of distinguishing the blood sample and the non-blood samples with respect to their optical properties. It is found that most of the analysis is able to separate the blood samples from the non-blood samples. The experiment conducted by using spectrophotometer suggests the ratio of reflected light at 700 nm to 630 nm as a parameter to separate the samples. It also suggests the ratio at 480 nm to 530 nm. The experiment with pulse oximeter suggests the ratio of transmitted light of red spectrum to that of infrared spectrum to separate the samples. In case of the RGB sensor, a function using two different channels of the RGB sensor can be used to separate the samples. The summary of the performance for all experiments is shown in Table 7-1.

.

Table 7-1: Summary of the experiments

Sensor	Measures	Parameter*	Cut-off value/s	Separation fails in the first dataset	Separation fails in the second dataset
Spectro-photometer	Reflection	Ratio (700 nm, 630 nm)	First dataset: 1.3664 Second dataset: 1.2093	NA	2NBS+ Swine blood: 0.04% to 6% Horse blood: 25% Hemoglobin solution: 18g/L
		Ratio (480 nm, 530 nm)	First dataset: 1.0095 Second dataset: 0.9189	NA	1NBS+ 0 BS
Pulse oximeter	Transmission	Ratio (Red, infrared)	First dataset: 101.1743 Second dataset: 101.0062	Horse blood: 8% Swine blood: 6% Hemoglobin:19.4g/L, 22.8g/L	(4NBS) + Hemoglobin solutions: 3g/L to 20g/L Swine blood: 0.04% to 2.0% Horse blood: 4%
RGB Sensor	Reflection	Intersection (Blue Red)	0	NA	1NBS+ NA
		Intersection (Green Red)	0	NA	1NBS+ NA
		Intersection (Blue Green)	0	4NBS+ 4BS Horse blood 50, 42, 25, 17	2NBS+ NA

*Parameter: Details are in corresponding chapters

7.2 Comparison

There are some studies about detection of bleeding using several optical sensors. The comparison among other works is shown in Table 7-2. The details can be found in the corresponding articles.

Table 7-2: Comparison among other works

Article cited	Sensor	Measures	Parameter	Cut-off value/s	BS	NBS	Fails to separate
[69]	TCS230D	Internal Reflection	Two factors		13 Hemoglobin	0	NA
[42]	TCS 3200	Internal reflection	HSL	H: 2 to 25 S:0.3 to 0.8	08 Normal human blood	02 Intestinal juice	Fails in low concentration Max/(128, 256, 512)
[65]	LED of Violet (415 nm) and red (720 nm)	Transmission Anchored in GI wall	Ratio	200	1	5	
[64]	LED (415,720)	Transmission	Ratio	50 (Approx)	Human blood 0.1%, 1%, 5%, 10%, 50%	19	Except 1% to 10% of Blood
[64]	Spectrophotometer	Transmission	Ratio	10000 (Aprox)	Human blood 0.1%, 1%, 5%, 10%, 50%	19	Except 1% to 10% of Blood
[66].	LED (415,720)	Transmission	Ratio	10	Human blood 5%, 7.7%, 13.3%, 15.4%, 33%, 40%	Water	

Here, only simple comparison among the previous research is presented. The dataset used in different studies were completely different hence, a quantitative comparison among the studies

is may lead to ambiguity. Detailed comparison of the works such as comparing the accuracy, specificity, sensitivity and few other statistical parameters are tough.

The comparison may focus only on few points such as the number of samples used, the validation of the proposed model, the region of operation, and the mode of operation. First of all, the number of samples used in this study is much more than any other previous works. Two different datasets were used where the first set contains 22 BS and 13 NBS, whereas the second set contains 43 BS with 23 NBS. Then, two different datasets were used in this study to validate the proposed technique, whereas no study had shown the validation using any second dataset. In addition, the sensors used in this study can detect any concentration of blood samples except very low concentration, which is similar to the previous works. However, the combination of different sensors can improve the detection. Finally, both transmission and reflection mode were used in this study as a result, the combination of all sensors is expected to detect different types of bleeding whereas the previous studies were performed only to detect acute bleeding.

Chapter 8 Conclusion and Future Works

The last chapter summarized the findings of the experiments using three different sensors and compared this work with other works done previously. This chapter will conclude the whole study and recommend for the future works

8.1 Conclusion

It can be concluded from the summary of the results that the optical sensors used in this study could be used to detect intestinal bleeding in the GI tract. The blood samples used in this study are not the human blood, rather those are horse blood, swine blood, and bovine hemoglobin. However, due to the similarities of the blood components, the same sensor and methods could be utilized to detect the human GI bleeding also.

The analysis of the samples with spectrophotometer suggest the ratio of ARL at two different pairs of wavelengths, (700 nm, 630 nm) and (480 nm, 530 nm). For both datasets, the cut-off value of the ratio is very close. The outcome of this analysis could be implemented by using light emitting diode and photodiode of the suggested wavelengths.

The Ratio of ATL of red light to infrared light also provides separation except for the very low concentration of blood samples. LED with the wavelength of corresponding red light and infrared light could be used to implement the outcomes in a capsule endoscopy.

The RGB sensor also provides good separation for all the three separating functions. This is a small sensor that might be possible to integrate within an endoscopy system.

The experiments presented in this study cover both reflection and transmission of light over the samples. Transmission of light could be utilized to detect active bleeding and reflection could be utilized to detect both active and old bleeding.

8.2 Recommendation for the Future Works

The recommendations for the future works to make the proposed design enhanced and suitable to detect the human GI bleeding could be as follows:

1. The in-vivo experiment should be performed. The experiments performed in this study are done in a controlled environment such as using a test tube and properly controlled orientation between samples and sensor. However, the situation would be different in the real scenario. Hence, the in-vivo test of samples using the sensors should be performed to confirm that the proposed sensors and the corresponding mode of operation for each sensor could be used in a living body.
2. Multiple sensors should be integrated into the capsule endoscopic system. The sensor, processor, communication module, and power modules are getting smaller and more efficient day by day [80]. Thus, integration of multiple sensors could be possible.
3. More features could be incorporated along with the current features to detect abnormalities of the GI tract. Sending thousands of images requires a huge amount of power. In this case, different sensors could be used to change the frame rate of transmission for example if there is any sign of abnormality detected by any sensors, the frame rate could be increased otherwise the frame rate may be reduced. This way, it could save the power consumption significantly. The saved power could be utilized by other modules for localization, hook-up, tissue collection, medicine injection and many other purposes.

References

[1] "Gastrointestinal (GI) Bleeding." Internet: https://www.niddk.nih.gov/health-information/digestive-diseases/gastrointestinal-bleeding, [Feb. 18, 2018].

[2] B. S. M. Kim *et al.*, "Diagnosis of gastrointestinal bleeding: A practical guide for clinicians," World J. Gastrointest. Pathophysiol., vol. 5, no. 4, pp. 467-478, Nov. 2014.

[3] M. C. Bateson and I. A. D. Bouchier, "Clinical Investigations in Gastroenterology." Gewerbestrasse Switzerland: Springer, 2017, pp. 2-5.

[4] D. Pryor *et al.*, Gastrointestinal Bleeding, Gewerbestrasse, Gewerbestrasse Switzerland: Springer, 2010.

[5] H. Z. Girgis *et al.*, "An intelligent system to detect Crohn's disease inflammation in Wireless Capsule Endoscopy videos," in *2010 IEEE International Symposium on Biomedical Imaging: From Nano to Macro*, Rotterdam, 2010, pp. 1373-1376.

[6] R. Kozarek and J. A. Leighton (2015), Endoscopy in Small Bowel Disorders. Internet: https://link.springer.com/book/10.1007%2F978-3-319-14415-3, [Feb. 18, 2018].

[7] B. Li et al, "Computer-aided small bowel tumor detection for capsule endoscopy," *Artif. Intell. Med.*, vol. 52, no. 1, pp. 11–16, 2011.

[8] G. Pan and L. Wang, "Swallowable wireless capsule endoscopy: Progress and technical challenges," *Gastroenterol. Res. Pract.*, vol. 2012, pp. 1-9, 2012.

[9] G. Iddan *et al*., "Wireless capsule endoscopy," *Gastrointest. Endosc.,* vol. 405, p. 417, May. 2000.

[10] Y. Yuan and M. Q. H. Meng, "Polyp classification based on Bag of Features and saliency in wireless capsule endoscopy," in *2014 IEEE International Conference on Robotics and Automation (ICRA)*, Hong Kong, 2014, pp. 3930-3935.

[11] R. Kumar *et al*., "Learning disease severity for capsule endoscopy images," in *2009 IEEE International Symposium on Biomedical Imaging: From Nano to Macro*, Boston, MA, 2009, pp. 1314-1317.

[12] Y. Yuan *et al.*, "Bleeding Frame and Region Detection in the Wireless Capsule Endoscopy Video," *IEEE J. Biomed. Heal. Informatics,* vol. 20, no. 2, pp. 624-630, Mar 2016.

[13] M. Keroack et al. (2004), Video capsule endoscopy., vol. 20, no. 5. Internet: http://www.springer.com/gp/book/9783662440612. [Feb. 18, 2018].

[14] Y. Fu et al., "Computer-aided bleeding detection in WCE video," *IEEE J. Biomed. Heal. Informatics*, vol. 18, no. 2, pp. 636–642, Mar. 2014.

[15] T. C. Lee *et al.*, "Computer-aided diagnosis in endoscopy: A novel application toward automatic detection of abnormal lesions on magnifying narrow-band imaging endoscopy in the stomach," *2013 35th Annual International Conference of the IEEE Engineering in Medicine and Biology Society (EMBC)*, Osaka, 2013, pp. 4430-4433.

[16] A. Hassan and M. Haque, "Computer-aided gastrointestinal hemorrhage detection in wireless capsule endoscopy videos," *Comput. Methods Programs Biomed.*, vol. 122, no. 3, pp. 341-353, Sep. 2015.

[17] K. Zadeh et al., "Ingestible Sensors," *ACS Sensors*, vol. 2, no. 4, pp. 468–483, 2017.

[18] P. C. De Groen, "History of the Endoscope [Scanning Our Past]," in *Proceedings of the IEEE*, vol. 105, no. 10, pp. 1987-1995, Oct. 2017.

[19] A. Ieva et al., “A journey into the technical evolution of neuroendoscopy,” *World Neurosurg.,* vol. 82, no. 6, pp. E777–E789, Dec. 2014.

[20] B. Krans, “Endoscopy: Purpose, Procedure & Types.” Internet: https://www.healthline.com/health/endoscopy, [Feb. 18, 2018].

[21] R. M. E. Engel, “Philipp Bozzini—The Father of Endoscopy,” *Journal of Endourology*, vol. 17, no. 10. pp. 859–862, 2003.

[22] “Bozzini and the Lichtleiter - Looking into the Body - Diagnosis - History of Urology - EAU European Museum of Urology.” Internet: http://history.uroweb.org/history-of-urology/diagnosis/looking-into-the-body/, [Feb. 18, 2018].

[23] H. H. Hopkins and N. S. Kapany, “A flexible fibrescope, using static scanning,” *Nature*, vol. 173, no. 4392, pp. 39–41, 1954.

[24] C Nezhat (2011), “Nezhat's History of Endoscopy”. Internet: http://laparoscopy.blogs.com/endoscopyhistory/chapter_08/, [Mar. 03, 2018].

[25] Z. Li et al.(2014), Handbook of capsule endoscopy, Springer Netherlands.

[26] H. Schwacha, “Capsule Endoscopy A guide to Becoming an Efficient and Effective Reader,” Springer International Publishing, 2017,

[27] L. J. Sliker and G. Ciuti, “Flexible and capsule endoscopy for screening, diagnosis and treatment,” *Expert Rev. Med. Devices*, vol. 11, no. 6, pp. 649–666, Nov. 2014.

[28] P. Valdastri, M. Simi, and R. J. Webster, “Advanced Technologies for Gastrointestinal Endoscopy,” *Annu. Rev. Biomed. Eng.*, vol. 14, no. 1, pp. 397–429, 2012.

[29] “Radio Pill.” *Nature*, Vol. 179, p. 898, 1957.

[30] S. C. Mukhopadhyay, "Wearable Sensors for Human Activity Monitoring: A Review," in *IEEE Sensors Journal*, vol. 15, no. 3, pp. 1321-1330, Mar. 2015.

[31] Douglas O. Faigel and David R. Cave, “Capsule endoscopy,” BMJ (Clinical research ed.), vol. 339. Elsevier, Philadelphia, United States, 2008.

[32] A. Uehara and K. Hoshina, “Capsule endoscope NORIKA system,” *Minim. Invasive Ther. Allied Technol.*, vol. 12, no. 5, pp. 227–234, Sep. 2003.

[33] K. Zhao, G. Yan, L. Lu, and F. Xu, “Low-Power Wireless Electronic Capsule for Long-Term Gastrointestinal Monitoring,” *J. Med. Syst.,* vol. 39, no. 2, pp. 1-9, Feb. 2015.

[34] A. Wang et al., “Wireless capsule endoscopy,” *Gastrointest. Endosc.*, vol. 78, no. 6, pp. 805–815, 2013.

[35] L. J. Sliker and G. Ciuti, “Flexible and capsule endoscopy for screening, diagnosis and treatment,” *Expert Rev. Med. Devices,* vol. 11, no. 6, pp. 649–666, Nov. 2014.

[36] CapsoVision, “Product Specifications.” Internet: http://www.capsovision.com/physicians/product-specifications, [Feb. 18, 2018].

[37] R. Scott and R. Enns, “Advances in capsule endoscopy,” *Gastroenterol. Hepatol.,* vol. 11, no. 9, pp. 612–617, Sep. 2015.

[38] M. Kanaan and H. Farhadi, “Advances in Wireless Video Capsule Endoscopy,” *Int. J. Wirel. Inf. Networks,* vol. 24, no. 2, pp. 166–167, Apr. 2017.

[39] W. G. Kwack and Y. J. Lim, “Current status and research into overcoming limitations of capsule endoscopy,” *Clin. Endosc.*, vol. 49, no. 1, pp. 8–15, Jan. 2016.

[40] A. Koulaouzidis *et al.*, “Wireless endoscopy in 2020: Will it still be a capsule?,” *World J. Gastroenterol.,* vol. 21, no. 17, pp. 5119–5130, May. 2015.

[41] C. V. de Bruaene *et al.,* “Small bowel capsule endoscopy: Where are we after almost 15 years of use?,” *World J Gastrointest Endosc,* vol. 7, no. 1, pp. 13–36, Jan. 2015.

[42] P. Qiao *et al.,* "A smart capsule system for automated detection of intestinal bleeding using HSL color recognition," PLoS One, vol. 11, no. 11, pp. 1–14, Nov. 2016.

[43] L. R. Fisher and W. L. Hasler, "New vision in video capsule endoscopy: current status and future directions," *Nat. Rev. Gastroenterol. Hepatol.,* vol. 9, no. 7, pp. 392–405, May. 2012.

[44] D. K. Iakovidis and A. Koulaouzidis, "Automatic lesion detection in wireless capsule endoscopy — A simple solution for a complex problem," *2014 IEEE International Conference on Image Processing (ICIP)*, Paris, pp. 2236-2240.

[45] H. O. Diaz Tartera *et al.,* "Validation of SmartPill ® wireless motility capsule for gastrointestinal transit time: Intra-subject variability, software accuracy and comparison with video capsule endoscopy," *Neurogastroenterol. Motil.,* vol. 29, no. 10, pp. 1-9, Oct. 2017.

[46] E. Grady, "Gastrointestinal Bleeding Scintigraphy in the Early 21st Century.," *J. Nucl. Med.*, vol. 57, no. 2, pp. 252–259, Feb. 2016.

[47] A. Zwart, "Spectrophotometry of hemoglobin: Various perspectives," *Clin. Chem.*, vol. 39, no. 8, pp. 1570–1572, Aug. 1993.

[48] M. Meinke *et al.,* "Chemometric Determination of Blood Parameters Using Visible – Near-Infrared Spectra," *Appl. Spectrosc.,* vol. 59, no. 6, pp. 826–835, Jun. 2005.

[49] M. Friebel *et al.,* "Determination of optical properties of human blood in the spectral range 250 to 1100 nm using Monte Carlo simulations with hematocrit-dependent effective scattering phase functions," *J. Biomed. Opt.,* vol. 11, no. 3, 9p. 034021–(1–10), May.-Jun. 2006.

[50] D. K. Sardar and L. B. Levy, “Optical Properties of Whole Blood,” *Lasers in Medical Science,* vol. 13, no. 2. pp. 106–111, Jun. 1998.

[51] N. Bosschaart *et al.,* “A literature review and novel theoretical approach on the optical properties of whole blood,” *Lasers Med. Sci.,* vol. 29, no. 2, pp. 453–479, Mar. 2014.

[52] F. J. Boehm, “Nanomedical Device and Systems Design: Challenges, Possibilities, Visions,” *CRC Press,* pp. 244–245, 2016.

[53] “Venous blood”, Internet: http://www.wiki30.com/wa?s=Venous_blood, [Feb. 18, 2018]

[54] B. Liu *et al.,* “Effects of haemodilution on the optical properties of blood during coagulation studied by optical coherence tomography,” *Quantum Electron.,* vol. 46, no. 11, pp. 1055–1060, 2016.

[55] I. R. Sinclair, “Sensors and Transducers,” 3rd Edition, Newnes, Oxford, 2001.

[56] B. G. Celler and R. S. Sparks, "Home Telemonitoring of Vital Signs—Technical Challenges and Future Directions," in *IEEE Journal of Biomedical and Health Informatics*, vol. 19, no. 1, pp. 82-91, Jan. 2015.

[57] Y. L. Zheng *et al*., "Unobtrusive Sensing and Wearable Devices for Health Informatics," in *IEEE Transactions on Biomedical Engineering*, vol. 61, no. 5, pp. 1538-1554, May 2014.

[58] C. Pang *et al*., “Recent advances in flexible sensors for wearable and implantable devices,” *J. Appl. Polym. Sci.*, vol. 130, no. 3, pp. 1429–1441, Jun. 2013.

[59] “Motility Monitoring, SmartPill,” Given Imaging, Internet: http://www.givenimaging.com/en-int/Innovative-Solutions/Motility/SmartPill/Pages/default.aspx, [Feb. 18, 2018].

[60] "CorTemp Sensor-HQInc." Internet: http://www.hqinc.net/cortemp-sensor-2/, [Feb. 18, 2018].

[61] "VitalSense Wireless Vital Signs Monitoring from Mini Mitter Company, Bend Oregon." Internet: http://www.temperatures.com/mmvs.html, [Feb. 18, 2018].

[62] B. Kuo et al., "Generalized transit delay on wireless motility capsule testing in patients with clinical suspicion of gastroparesis, small intestinal dysmotility, or slow transit constipation," *Dig. Dis. Sci*., vol. 56, no. 10, pp. 2928–2938, Oct. 2011.

[63] K. Tran *et al.,* "Evaluation of regional and whole gut motility using the wireless motility capsule: Relevance in clinical practice," *Therap. Adv. Gastroenterol*., vol. 5, no. 4, pp. 249–260, Jul. 2012.

[64] S. Schostek *et al.,* "Telemetric real-time sensor for the detection of acute upper gastrointestinal bleeding," *Biosens. Bioelectron.,* vol. 78, pp. 524–529, Apr. 2016.

[65] S. Schostek and M. O. Schurr, "The HemoCop Telemetric Sensor System- Technology and Result of in-vivo Assessment." *Stud Health Technol Inform.*, vol. 177, pp. 97–100, 2012.

[66] S. Schostek et al., "Volunteer Case Series of a New Telemetric Sensor for Blood Detection in the Upper Gastrointestinal Tract: The HemoPill," *Dig. Dis. Sci*., vol. 61, no. 10, pp. 2956–2962, Oct. 2016.

[67] W. X. Wang, G. Z. Yan, F. Sun, P. P. Jiang, W. Q. Zhang, and G. F. Zhang, "A non-invasive method for gastrointestinal parameter monitoring," *World J. Gastroenterol.,* vol. 11, no. 4, pp. 521–524, Jan. 2005.

[68] C. J. Bettinger, "Materials Advances for Next-Generation Ingestible Electronic Medical Devices," *Trends Biotechnol*., vol. 33, no. 10, pp. 575–585, Oct. 2015.

[69] H. Liu et al., “An intelligent electronic capsule system for automated detection of gastrointestinal bleeding,” *J. Zhejiang Univ. Sci. B*, vol. 11, no. 12, pp. 937–943, Dec. 2010.

[70] S. L. Gorbach, “Microbiology of the Gastrointestinal Tract - Medical Microbiology,” *NCBI Bookshelf,* 2017.

[71] “Spectrophotometry- Handbook”, GE Healthcare Life Sciences, Internet: https://www.sigmaaldrich.com/content/dam/sigma-aldrich/docs/Sigma-Aldrich/General_Information/1/ge-spectrophotometry.pdf, [Feb. 18, 2018].

[72] S. J. Tavener and J. E. Thomas-oates, “Build your own spectrophotometer,” *Educ. Chem.*, vol. 44, no. 5, pp. 151–154, 2007.

[73] “Portable Spectrophotometers-Konica Minolta Sensing." Internet: http://sensing.konicaminolta.us/technologies/portable-spectrophotometers/, [Feb. 18, 2018].

[74] “Field-oriented spectrophotometer for reliable color measurement.” Konica Minolta, Spectrophotometer CM-700d/600d.

[75] “Color spectrophotometer / portable / sphere / for color measurement.” Internet: http://www.directindustry.com/prod/konica-minolta/product-18413-1031579.html, [Feb. 18, 2018].

[76] “Spectrophotometer 700d/600d Instruction Manual,” Konica Minolta, Spectrophotometer CM-700d/600d.

[77] “Nellcor Spo2 Finger Probe.” Internet: https://coastbiomed.com/product/nellcor-spo2-finger-probe/, [Feb. 18, 2018].

[78] “SPO2 Sensor Probe for Pulse Oximetry." Internet: https://www.sunrom.com/p/spo2-sensor-probe-for-pulse-oximetry, [Feb. 18, 2018].

[79] “HDJD-S822-QR999 RGB Color Sensor Data Sheet,” AVAGO TECHNOLOGIS, 2007.

[80] A. Kiourti and K. S. Nikita, “A review of in-body biotelemetry devices: Implantables, ingestibles, and injectables,” *IEEE Trans. Biomed. Eng.,* vol. 64, no. 7, pp. 1422–1430, Jul. 2017.